



Universidade de Aveiro Departamento de Biologia

2016

JULIANE OLIVEIRA VIÉGAS **Potencial Citotóxico do Óxido de Grafeno em Células Tumorais do Pulmão Humano**

Cytotoxic Potential of Graphene Oxide in Human Lung Adenocarcinoma Cell Line

DECLARAÇÃO

Declaro que este relatório é integralmente da minha autoria, estando devidamente referenciadas as fontes e obras consultadas, bem como identificadas de modo claro as citações dessas obras. Não contém, por isso, qualquer tipo de plágio quer de textos publicados, qualquer que seja o meio dessa publicação, incluindo meios eletrônicos, quer de trabalhos acadêmicos.



Universidade de Aveiro Departamento de Biologia

2016

**JULIANE OLIVEIRA
VIEGAS**

**Potencial Citotóxico do Óxido de Grafeno em Células
Tumorais do Pulmão Humano**

Cytotoxic Potential of Graphene Oxide in Human Lung Adenocarcinoma Cell Line

Dissertação apresentada à Universidade de Aveiro para cumprimento dos requisitos necessários à obtenção do grau de Mestre em Biologia Molecular e Celular, ramo da Biologia, realizada sob a orientação científica da Doutora Helena Cristina Correia de Oliveira, Investigadora de Pós-doutoramento do Departamento de Biologia e do Centro de Estudos do Ambiente e do Mar – CESAM da Universidade de Aveiro.

Apoio financeiro da Fundação para a Ciência e Tecnologia (FCT) pelo projeto ERA--SIINN/0003/2013 e do CESAM (Ref. FCT UID/AMB/50017), por parte da FCT/MEC através de fundos nacionais, e pelo cofinanciamento pelo FEDER, no âmbito do Acordo de Parceria PT2020 e Compete 2020.



UNIÃO EUROPEIA
Fundo Europeu
de Desenvolvimento Regional

FCT Fundação para a Ciência e a Tecnologia
MINISTÉRIO DA CIÊNCIA, TECNOLOGIA E ENSINO SUPERIOR

Dedico este trabalho aos meus amados pais, pelo incansável apoio e compreensão perante a minha longa ausência, por todo o amor e orações que sem dúvida fizeram grande diferença para realização dessa etapa da minha trajetória. Por fim, e o mais importante, a Deus, a quem estive e está a guiar o meu caminho.

o júri

presidente

Doutora Helena Silva

Professora Auxiliar do Departamento de Biologia da Universidade de Aveiro.

Arguente principal

Doutora Mónica Cicuéndez Maroto

Investigadora em Pós-Doutoramento, Departamento de Engenharia Mecânica, CICECO & NRD-TEMA.

Orientadora

Doutora Helena Cristina Correia de Oliveira

Investigadora Pós-Doutoramento, CESAM - Centro de Estudos do Ambiente e do Mar da Universidade de Aveiro

Agradecimentos

Primeiramente gostaria de agradecer a minha orientadora Doutora Helena Oliveira por ter me proporcionado essa grande oportunidade em participar desse projeto de investigação. Pela atenção desprendida em invariáveis momentos e disponibilidade em orientação, a senhora consistentemente permitiu-me trabalhar com independência, do mesmo modo, sempre se demonstrou disponível para atender qualquer dúvida que eu viesse a ter. Agradeço muitíssimo a sua paciência e compreensão. Agradeço carinhosamente a minha parceira de Lab, Débora Reis, por todo suporte e ajuda, para além da amizade que criamos, agradeço muitíssimo pelos conselhos, almoços, lanches e tarefas que compartilhamos. Saiba que sempre poderás contar comigo dentro ou fora de um laboratório. As demais colegas do laboratório, Catarina e Ana que estiveram sempre disponíveis em ajudar, um agradecimento especial a Maryam, Fernanda e Joana, que estiveram logo no início da minha jornada no Lab e ajudaram-me na minha ambientação com as rotinas do laboratório. Agradeço ao Ricardo Pinto, do departamento de química da Universidade de Aveiro pela ajuda e disponibilização para que assim fosse possível realizar o parâmetro de caracterização das nossas nanopartículas. De uma forma especial, agradeço as minhas colegas de casa, que de fato, se tornaram a minha família aqui em Portugal, com certeza guardarei para sempre os preciosos momentos que tivemos e todas as emoções e cardápios que compartilhamos. Obrigada Evelyn pelo exemplo de pessoa que és, e pela sua amizade que foi além de um simples “Free hug” no meio da rua em 2014. Rose, obrigada pela atenção e ajuda sempre presente. Adriana, a minha melhor flatmate portuguesa, obrigada por todo carinho. Aos demais amigos que a Universidade de Aveiro me presenteou: Diana, Andreia, Ana Patrícia, Liege, Niedja e outros, muito obrigada pelo apoio e pelos convívios sempre necessários quando tudo parecia ser difícil demais. Agradeço aos meus amigos da Igreja Adventista do Sétimo Dia que congreguei durante a minha estadia em Aveiro. Um “muito obrigada” a aqueles que me apoiaram em diversas maneiras, antes mesmo de decidir fazer o mestrado em Portugal, aos amigos queridos da Irlanda e do Brasil que me deram forças para seguir o meu sonho. Finalmente, gostaria de expressar a minha profunda gratidão aos meus pais por providenciarem todo suporte financeiro e encorajamento ao longo desses anos longe de casa, tudo isso para me proporcionar a realização de um sonho, que foi além de um simples intercâmbio de 6 meses, foi um mestrado, foi um amadurecimento e crescimento sem igual. As minhas irmãs Karoline e Allyne, ao meu irmão André, que tanto sinto falta, aos meus cunhados Walter e Thiago, acreditem, nada disso seria realizado sem o suporte de vocês, pois mesmo sentindo a dor da saudade, nunca deixaram de me apoiar. Amo todos vocês.

palavras-chave

Óxido de grafeno; citotoxicidade; A549; viabilidade celular; espécies reativas de oxigênio (ROS); citometria de fluxo.

resumo

O óxido de grafeno (GO) é um composto com aplicação em diversas áreas, especialmente biomedicina e ambiente, devido as suas propriedades únicas que lhe conferem excelentes características. Apesar da atual ampla utilização de nanomateriais, a falta de informação sobre os riscos para a saúde humana e para o ambiente ainda permanece. Consequentemente, a investigação sobre a toxicidade das nanopartículas deve ser uma prioridade. Sendo o pulmão uma das principais vias de entrada das nanopartículas no organismo, o objetivo deste trabalho é avaliar o potencial citotóxico de óxido de grafeno no pulmão, usando como modelo uma linha celular epitelial de carcinoma do pulmão humano (A549). A morfologia e a viabilidade das células A549 foram avaliados após 24 horas de exposição a concentrações de GO entre 10µg/mL a 200µg/mL. A captação de GO e a produção de espécies reativas de oxigênio foram avaliadas por citometria de fluxo. Os resultados sugerem que GO não apresenta óbvia toxicidade para as células A549, quando avaliada pelo ensaio WST-8. No entanto, no ciclo celular observou-se uma ligeira alteração na fase S e na fase G2 em 50µg/mL, com paragem na fase G2. GO induziu também um aumento na produção de ROS em doses mais baixas (10µg/mL e 37µg/mL). A captação intracelular de GO aumentou para a dose mais elevada. Em conjunto, estes resultados sugerem que esta forma de GO apresenta biocompatibilidade para as células de pulmão.

Keywords

Graphene oxide; cytotoxicity; A549; cell viability; reactive oxygen species (ROS); Flow Cytometry.

abstract

Graphene oxide (GO) is a compound with application in several fields, especially biomedicine and environment, due to its unique properties which confer excellent characteristics. Despite the nowadays wide application of nanomaterials, the lack of information regarding the risks to human health and the environment is still remaining. Consequently, the investigation about the toxicity of nanoparticles must be a priority. The lung is one of the main routes of entry for nanoparticles into the body, therefore, the aim of this study is to evaluate the cytotoxic potential of graphene oxide in lung, using as model the human carcinoma epithelial cell line (A549). The morphology and viability of A549 cells were evaluated after 24h of exposure to GO at concentrations from 10 μ g/ml to 200 μ g/ml. The uptake of GO and the production of reactive oxygen species were also investigated by flow cytometry. The results suggest that GO has no obvious toxicity to A549 cells when assessed by WST-8 assay, though the cell cycle showed a slightly alteration in the S and G2 phase at 50 μ g/mL with arrest at G2 phase. Also, GO showed an increasing in the ROS production at the lowest doses (10 μ g/mL and 37 μ g/mL). The intracellular uptake increased for the highest concentration. Together these results suggest that this form of GO shows biocompatibility for lung cells.

List of Tables and Figures

TABLE 1. PHYSICO-CHEMICAL NP PROPERTIES OF RELEVANCE FOR TOXICOLOGY. ADAPTED FROM OBERDÖRSTER, 2010.	2
FIGURE 1. GENERAL PROPERTIES OF GRAPHENE ON THE LEFT HAND SIDE AND THE MAIN APPLICATION AREAS OF GRAPHENE ON THE RIGHT HAND SIDE (LIU ET AL., 2013; NGUYEN AND ZHAO, 2014; SUN ET AL., 2008).	3
FIGURE 2. STRUCTURE OF GRAPHENE, GRAPHENE OXIDE AND REDUCED GRAPHENE OXIDE. ADAPTED FROM PERREAULT ET AL., 2015.	4
FIGURE 3. PRODUCTION OF GRAPHENE OXIDE FROM OXIDATIVE METHODS ON GRAPHITE MATERIAL. SCHEME ADAPTED FROM LAY ET AL., 2013.	5
FIGURE 4. SCHEME OF GENERAL POSSIBILITY OF NANOPARTICLES (NPs) REACH THE BODY.	7
FIGURE 5. ABSORPTION OF NANO-SIZED PARTICLES. SHOWING ROUTES OF EXPOSURES, THE MAIN UPTAKE PATHWAYS, METABOLISM AND EXCRETION OF NPS (OBERDÖRSTER ET AL., 2005).	8
FIGURE 6. PRINCIPLE OF CELL VIABILITY DETECTION BY WST-8 ASSAY. THE WST-8 REAGENT IS ADDED TO CELLS AND THE ELECTRON MEDIATOR RECEIVES ELECTRONS FROM A VIABLE CELL (NADH ENZYME) AND TRANSFERS THE ELECTRON TO WST-8 IN THE CULTURE MEDIUM WHICH IS REDUCED, RESULTING IN AN ORANGE-COLOURED PRODUCT (FORMAZAN).	12
FIGURE 7. CELL CYCLE CHECKPOINT PATHWAYS IMPINGING UPON THE CELL DIVISION CYCLE. ILLUSTRATION FROM CHIN AND YEONG, 2010.	14
FIGURE 8. HISTOGRAM OF CELL CYCLE. DISTRIBUTION OF THE CELLS IN DIFFERENT PHASES OF CELL CYCLE.	15
FIGURE 9. SCHEMATIC OF A FLOW CYTOMETER. (RILEY AND IDOWU, 2009)	15
TABLE 2. ZETA POTENTIAL OF GRAPHENE OXIDE IN THE CULTURE MEDIUM AND MILLIQ WATER. THE SAMPLES WERE ANALYSED BY DLS AND THE DATA ARE EXPRESSED AS MEANS \pm SD OF THREE DIFFERENT SCANS.	22
FIGURE 10. SIZE DISTRIBUTION OF GO (INTENSITY). SAMPLES WERE SUSPENDED IN MILLI Q WATER AND F12-K MEDIUM AT CONCENTRATION OF 10 μ G/ML AND ASSESSED BY TIME (0H, 2H, 4H AND 24H) THE Z-AVERAGE SIZE THROUGH DLS. DATA ARE EXPRESSED AS MEAN \pm SD.	23
TABLE 3. AVERAGE HYDRODYNAMIC DIAMETER (INTENSITY) OF GO AND THE POLYDISPERSITY INDEX (PDI) VALUES. GRAPHENE OXIDE DILUTED IN WATER AND F12-K MEDIUM (10 μ G/ML).	23
FIGURE 11. SIZE DISTRIBUTION (BY INTENSITY) REPORT OF DLS MEASUREMENTS. A. GO DISPERSION IN MILLI Q WATER (0H) AND B. GO DISPERSION IN F12-K MEDIUM.	24
FIGURE 12. SIZE DISTRIBUTION (NUMBER) OF GO IN MILLI Q WATER AND (*) F-12K MEDIUM AT CONCENTRATION OF 10 μ G/ML ACCORDING TO INCUBATION TIME. DATA ARE EXPRESSED AS MEANS \pm SD.	24
FIGURE 13. LIGHT MICROSCOPY IMAGES OF A549 CELLS. CONFLUENCE SURFACE OF A549 CELLS; LEFT: CELLS AT 10X MAGNIFICATION; RIGHT: CELLS AT 40X MAGNIFICATION.	25
FIGURE 14. LIGHT MICROSCOPY IMAGES OF A549 CELLS EXPOSED TO GO AFTER 24H. A - CONTROL CELLS; B - 10 μ G/ML; C - 150 μ G/ML BEFORE AND AFTER THE WASHING PROCESS WITH PBS, SHOWN THE AFTER WASHING PROCESS IN THE UPRIGHT IMAGE. INSERT AT 10X MAGNIFICATION.	25
FIGURE 15. OPTIMIZATION OF WST-8 ASSAY. PERFORMED WITH 2 CELL DENSITIES (5 \times 10 ³ AND 7 \times 10 ³); THE INCUBATION TIME WERE 1H, 2H AND 3H AND 4 H (DATA NOT SHOWN).	26
FIGURE 16. WST-8 ASSAY WAS PERFORMED AFTER A549 CELLS (7 \times 10 ³) WERE EXPOSED FOR 24 HOURS TO GO. THE CELLS WERE NOT SUBMITTED TO THE PBS WASHING STEP IN THIS ASSAYS (N=3). THE GREEN ARROW INDICATES THE ABSORBANCE FOUND ON THE GO AND WST-8 REAGENT ONLY. DATA IS SHOWED AS MEAN \pm SD.	27
FIGURE 17. CELL VIABILITY OF A549 CELLS EXPOSED TO GO IN INCREASE CONCENTRATIONS. WST-8 ASSAY WAS EVALUATED AND STATISTICAL ANALYSIS WAS PERFORMED WITH ANOVA. MEANS \pm SD N=3.	27
FIGURE 18. CELL VIABILITY ASSAY OF A549 CELLS 7 \times 10 ³ EXPOSED TO GO-FREE MEDIUM IN INCREASE CONCENTRATIONS. WST-8 ASSAY WAS EVALUATED AND STATISTICAL ANALYSIS WAS PERFORMED WITH ANOVA (P<0.05). MEANS \pm SD N=2.	28
FIGURE 19. LEVEL OF INTRACELLULAR ROS UPON EXPOSURE TO GO. A549 CELLS WERE EXPOSED TO INCREASING CONCENTRATIONS OF GO AND MEASURED BY FCM. (*) SHOWS THE STATISTICALLY SIGNIFICANT DIFFERENCE (P<0.001). DATA SHOWS MEANS \pm SD.	29
FIGURE 20. CELL CYCLE RESULTS OF A549 GO EXPOSURE AFTER 24H. THE GIVEN RESULTS ARE THE MEAN % OF CELL POPULATION (\pm SD) ALONG CELL CYCLE STAGES. (*) SHOWS THE STATISTICALLY SIGNIFICANT DIFFERENCE (P=<0,001) WITH MULTIPLE COMPARISONS VERSUS CONTROL GROUPS.	30
FIGURE 21. PERCENTAGE OF CELLS IN EACH PHASE OF THE CELL CYCLE UPON EXPOSURE TO GO FOR 24H. WHERE (*) SHOWS THE STATISTICALLY SIGNIFICANT DIFFERENCE WITH P<0.05. HISTOGRAMS ARE SHOW FROM CONTROL CELLS AND GO (50 μ G/ML) TREATED CELLS.	31

FIGURE 22. UPTAKE OF GO IN A549 CELLS INCUBATED AT 37°C (LEFT HAND SIDE) AND 4°C (RIGHT HAND SIDE). (*) SHOWS THE STATISTICALLY SIGNIFICANCE DIFFERENCE FOUND UPON EXPOSURE TO GO (P<0.05). MEANS ±SD, N=2.32

List of Acronymes and Abbreviations

A549 – Human lung adenocarcinoma cell line

DCFH-DA - 2'-7'-Dichlorodihydrofluorescein Diacetate

Dh - Hydrodynamic diameter

DLS – Dynamic Light Scattering

F-12K - Kaighn's Modification of Ham's F-12 Medium

FBS – Fetal Bovine Serum

FCM – Flow Cytometry

FS – Forward Scatter

GFNs – Graphene-Family Nanomaterials

WST-8 – Water-Soluble Tetrazolium Salt

GO – Graphene Oxide

MTT – Methylthiazolyldiphenyl-Tetrazolium Bromide

PBS – Phosphate Buffer Saline

PDI – Polydispersity Index

PI – Propidium Iodide

ROS – Reactive Oxygen Species

SS – Side Scatter

Table of contents

I. INTRODUCTION	1
I.1 NANOSCIENCE	1
I.2 NANOTOXICOLOGY	1
I.3 GRAPHENE NANOPARTICLES.....	3
I.3.1 Graphene Overview	3
I.3.2 Graphene Oxide Description	4
I.3.3 Application of Graphene Oxide	5
I.3.4 Potential for Human Exposure	7
I.4 NANOTOXICITY STUDIES	8
I.5 TOXICITY AND BIOCOMPATIBILITY	9
II. PRINCIPLES OF METHODS EMPLOYED	11
II.1 CHARACTERIZATION OF NANOMATERIALS	11
II.2. IN VITRO TOXICITY ASSESSMENT.....	11
II.2.1 Cell line and treatment	11
II.2.2 Cell Viability.....	12
II.2.3 Reactive Oxygen Species	13
II.2.4 Cell cycle analysis	14
II.2.5 Flow Cytometry – FCM.....	15
III. AIMS	17
IV. EXPERIMENTAL PROCEDURES	18
IV.1 GRAPHENE OXIDE MATERIAL	18
IV.2 CHARACTERIZATION OF GRAPHENE OXIDE	18
IV.2.1 Dynamic Light Scattering – DLS.....	18
IV.3 CELL LINE CULTURE AND TREATMENT.....	18
IV.4 CELL VIABILITY ASSAY: WST-8.....	19
IV.5 DETERMINATION OF REACTIVE OXYGEN SPECIES.....	19
IV.6 CELL CYCLE ANALYSIS.....	20
IV.7 INTRACELLULAR UPTAKE.....	20
IV.8 STATISTICAL ANALYSIS.....	21
V. RESULTS	22
V.1 CHARACTERIZATION OF GO	22
VI.1 Zeta Potential.....	22
VI.2 Size distribution and Polydispersity Index (PDI)	22
V.2 MORPHOLOGY OF A549.....	25
V.3 CELL VIABILITY – WST-8	26
V.4 DETERMINATION OF REACTIVE OXYGEN SPECIES	29
V.5 CELL CYCLE ANALYSIS	30
V.6 UPTAKE OF GO	32
VI. DISCUSSION	33
VII. CONCLUSION AND FUTURE PERSPECTIVES	37
VIII. REFERENCES	38

I. Introduction

I.1 Nanoscience

Nanoscience and nanotechnology are placed in the greater technological area, as the science has advanced throughout the time in many areas, the “nano” field also has evolved and expanded quickly. Attention has been driving to this field as long as the nanomaterials have shown great potential application in several areas of science ranging from medicine, food processing, to energy production and storage, and electronics (Agrawal, 2013). This promising field deals with materials with structures that reveal distinctive physical, chemical and biological properties due to their nanoscale. They have unique optical, magnetic, and mechanical properties and a large surface area (Beer et al., 2012).

Nanomaterials are defined by the International Organization for Standardisation - IOS, as a natural, incidental or manufactured material containing particles with at least one of its dimensions at 100nm or less (European Commission, 2011). Nanoparticles are also classified based on their dimensionality (1D, 2D or 3D), morphology, composition, uniformity and agglomeration. Nanoparticles may be formed naturally through numerous physical processes from erosion to combustion, whereby this leads to health risks reaching from harmful to benign responses (Buzea et al., 2007). The use of nanoparticles has facilitated the emergence of innovative products in areas such as electronic, medicine, biotechnology, industry, among others (Ai et al., 2011). With this large spectrum of application, the nanoscience might reach the common industry with products with more efficacy, quality, more environmental sustainable and maybe less cost.

The work in nanoscience and nanotechnology has also brought new perspectives to overcoming challenges at the nano scale. As more approaches from different areas of research have worked in this field, the possibility of those variable nanomaterials be more available in a common society has also increased. This process leads to an essential matter, the safety level of nanomaterials.

I.2 Nanotoxicology

Despite the promising future of the nanomaterials, it is known that its use brings risks and potential harmful impacts on human health and the environment. The physical and chemical properties of NPs have been recognized as the main reason for the impact in the biological and toxicological activity. As the table 1 shows, there are many physico-chemical properties of relevance for toxicology properties and their measurement are important for the

understanding of toxicological results (Oberdorster, 2010). As a major issue, an assessment of the toxicological and ecotoxicological risks should take into account these properties, especially in regard to the nanomaterial production when considered at the industrial level (Ai et al., 2011; Buzea et al., 2007). There is a great development in the biomedical context, where the nanoparticles with their unique properties and features can have high application in the biomedical field. However, it is important to mention once more the potential adverse effects that are unknown in the use of nanoparticles (Fadeel et al., 2010; Oberdorster, 2010). With the lack of information, many questions arise about the interaction of nanoparticles with biological systems. Despite nanomedicine advances in diagnostic and therapeutic systems, the potential effect on human health due to constant exposure to nanomaterials has not been completely unveiled (Cancino et al., 2014; Pyrrho and Schramm, 2012), therefore, systematic evaluations of the potential toxicity of nanomaterials should be urgently conducted.

Table 1. Physico-chemical NP properties of relevance for toxicology. Adapted from Oberdorster, 2010.

Physico-chemical NPs properties of relevance for toxicology	
Size (airborne, hydrodynamic) Size distributions Shape Agglomeration/aggregation Surface properties <ul style="list-style-type: none"> ○ Area (porosity) ○ Charge ○ Reactivity ○ Chemistry (coatings, contaminants) ○ Defects Solubility (lipid, aqueous, <i>in vivo</i>) Crystallinity	<div style="text-align: center;">Properties can change</div> <ul style="list-style-type: none"> • with method of production preparation process storage. • when introduced into physio, media, organism.

Nanotoxicology is proposed as a new subject in the toxicology area to investigate specifically the adverse effects caused by nanomaterials on the way to contribute to the development of a sustainable and safe technology (Donaldson et al., 2004). Understanding the characteristics such as dispersion, accumulation, stability and agglomeration level becomes essential to characterize the nanoparticle in order to meet its biocompatibility (Ai et al., 2011). Likewise, obtained knowledge will perform an important part in efficacy, safety and regulatory consent for materials, diagnostics and therapeutics.

I.3 Graphene Nanoparticles

I.3.1 Graphene Overview

Graphene is a two-dimensional carbon crystal composed of a single layer and hexagonally arranged carbon atoms. The assembling of its layers constitute the graphite that is a material existing in nature. In 2010 the Nobel Prize in Physics was given to two researchers Konstantin Sergeevich Novoselov and Andre Geim Konstantinovich both from University of Manchester, who successfully isolated for the first time in 2004 the material in its free state by a mechanical exfoliation from graphite crystal (Geim and Novoselov, 2007; Novoselov et al., 2004). Since there, studies with graphene and its derivatives were intensified and unique properties were discovered.

Theoretically, the material has been studied for a long period, however in practical ways, just in 2004 after the efficient isolation of graphene by (Novoselov et al., 2004), it came a flourishing time to graphene. Assuming the discovering of the very exclusive properties of graphene, it may be highlighted: the large surface area; chemical and mechanical stability; high electrical and thermal conductivity; and good biocompatibility (Geim, 2009; Kuila et al., 2012; Liu et al., 2013), all these features have given more focus to the material to be applied in many areas of science (Figure 1).

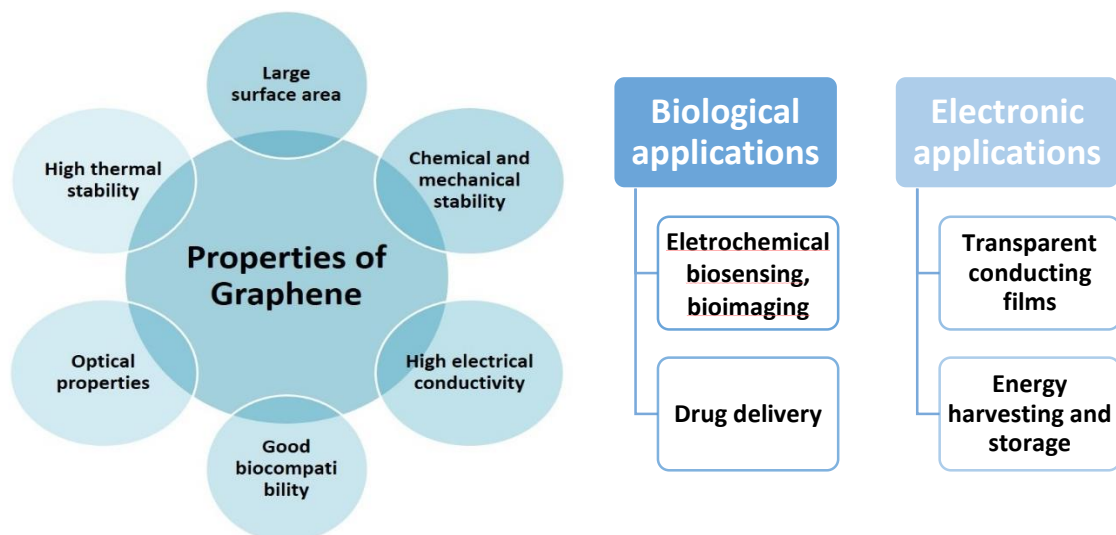


Figure 1. General properties of graphene on the left hand side and the main application areas of graphene on the right hand side (Liu et al., 2013; Nguyen and Zhao, 2014; Sun et al., 2008).

Sanchez et al. 2013 proposed a systematic nomenclature for the derivatives of graphene as Graphene-Family Nanomaterials (GFNs) and those materials are: few-layer graphene (FLG), graphene oxide (GO), reduced graphene oxide (rGO), ultrafin graphite, and

graphene nanosheets (GNS), (Sanchez et al., 2013). The scope of areas which GFNs can be applied, its ranging from nano-electronic to biomedical field and those nanoparticles have attracted a vast interest both in academics and industry. It is also known that all the unique properties of graphene, are associated with its individual sheet (Kuila et al., 2012; Li et al., 2008), however so many difficulties have been found to produce a functionalized single-layer graphene in bulk scale. The main reason is the aggregation/agglomeration tendency (Kuila et al., 2012) of its layers for the presence of hydrophobic nature (Kiew et al., 2016) nonetheless, many studies have been done to find a way to overcome this challenge (Li et al., 2008; Zhang Liu et al., 2008; Shan et al., 2009).

Over the years, GO has become a favourite graphene's derivative for the functionalization of graphene, mainly regard the solubility that is limited by graphene and in part for GO. Once the graphene is highly hydrophobic and does not have oxygen-containing groups as the GO owns, this confers to GO a better dispersion in water solution that represent a potential in the medicine and industry applications. In spite of the solubility of GO in water, it exhibits aggregation in variable mediums (Liu et al., 2013; Zhang et al., 2016; Zhou and Gao, 2014).

1.3.2 Graphene Oxide Description

Graphene oxide material consists of single-atom-thick carbon sheets with hydrophilic peripheral groups (carboxylate groups) that offer colloidal stability. In the basal surface, GO also shows uncharged polar groups (hydroxyl and epoxide) as well is found hydrophobic graphenic domains and capable of π - π interactions for drug loading and others functionalization (Cote et al., 2010; Park et al., 2009) (Figure 2). Above all, these groups allow this material to be functionalized by covalent and non-covalent methods (Dreyer et al., 2009). All this structure makes GO as an amphiphilic sheet-like molecule, which can show an excellent

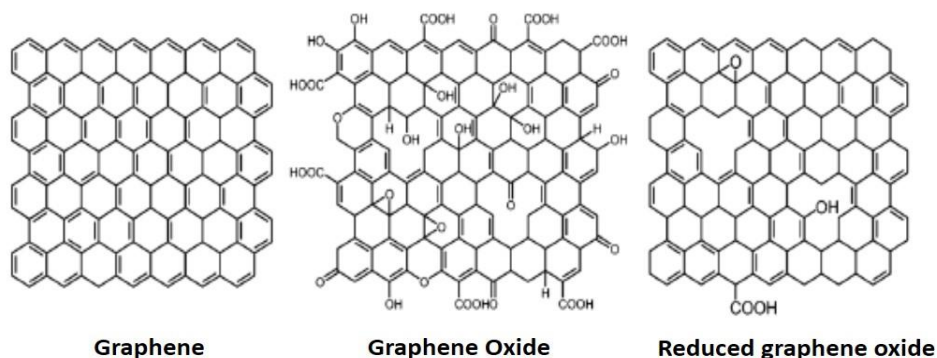


Figure 2. Structure of graphene, graphene oxide and reduced graphene oxide. Adapted from Perreault et al., 2015.

ability as surfactant, used to stabilize hydrophobic substances in water solutions (Cote et al., 2010).

GO as a highly oxidized form of a modified graphene, might contain not only monolayers but multilayer flakes, for that reason is required a complete characterization of the material (Sanchez et al., 2013) to guarantee a systematic and comprehensive study. Moreover, the variation of the material such as the characteristic in number of layers, size, chemical structures are already recognized to be involved in the toxicity of the material likewise, the different methods of producing graphene oxide (Lay et al., 2013; Seabra et al., 2014).

Nowadays GO can be easily prepared and the most common method is the procedure described by Hummers and Offeman, 1958. There are four main used methods to produce GO: Hoffman; Staudenmaier; Tour; and Hummers; all these methods use different oxidative methods of graphite to GO preparation and generally they all produce GO with similar properties (figure 3). From the idea of this variation on the oxidative conditions, it is expected the difference among the amounts of oxygen functionalities present on GO (Dreyer et al., 2009; Lay et al., 2013).

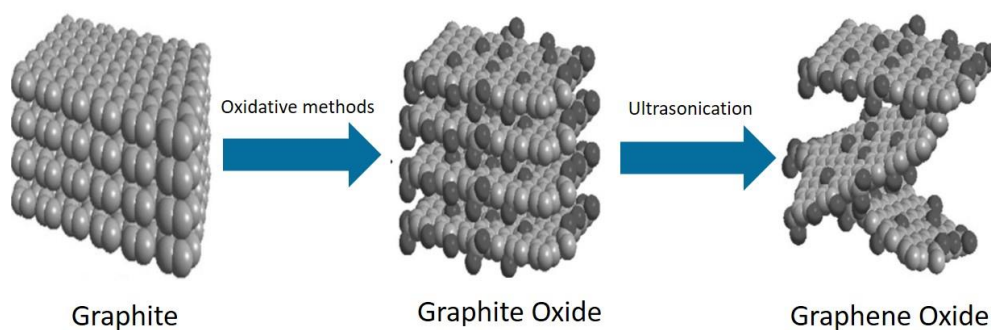


Figure 3. Production of Graphene Oxide from oxidative methods on graphite material. Scheme adapted from Lay et al., 2013.

I.3.3 Application of Graphene Oxide

Graphene oxide, as a prominent derivative of graphene, has hold numerous and promising advantages in different areas, including electronic, mechanical, medical and environmental fields (Liu et al., 2013; Sun et al., 2008). Regarding the potential of GO, a number of groups have dedicated their efforts to GO-based materials.

In the biomedical and environmental field, GO has been increasingly used showing great potential and promising results. For example, in biomedical application GO has been studied as an excellent drug-delivery, when in a pioneer work (Zhuang Liu et al., 2008) it was used polyethylene glycol (PEG) associated with GO, as a nanocarrier of a water-insoluble anticancer drugs and their results revealed a superior increase on the solubility and a great anticancer efficacy with the camptothecin analog SN38 drug. In another study, GO demonstrated to be a good carrier of doxorubicin (DOX) into cancer cells, once this drug is well known to have a potential anticancer agent, also is related with some adverse effects when used by itself. However, this association DOX-GO, was suggested to be used for therapeutic purpose (Yang et al., 2008); also for treatment of drug-resistant cancers, as it was found when anthracycline antibiotic (ADR) was loaded onto GO and this association showed a greater effect against breast cancer cells (MCF-7), which cells are known to be resistant to ADR by itself (Wu et al., 2012). Moreover, GO has shown potential for loading different molecules beyond GO-DOX, which has been extensively studied (Lv et al., 2016; A. J. Shen et al., 2012; Yang et al., 2008), but also with small molecules such as proteins, where GO-PEG was related for the first time to be used as an very effective nanovector for delivery proteins into cells, being used as a protection to avoid the protein to be hydrolysed enzymatically (H. Shen et al., 2012), still GO is related to be associated with peptides (Shim et al., 2015) and nucleic acids (Lu et al., 2009). As other ways to apply GO in the biomedical field, instead of drug-loading or nanocarrier there are also studies relating great potential in bioanalysis; disease-related diagnostics, near-infrared phototherapy and imaging (Feng et al., 2013; Shi et al., 2014).

The applications of GO in the environment have been also increasing. Studies related to the application of the nanomaterial directly, for example in 2013 was found that GO would be stable in an aquatic environment (Chowdhury et al., 2013), also GO was investigated in a way to create a biofoam to clean dirty water and this promising method combines bacteria-produced cellulose and GO to form a bilayered biofoam (Jiang et al., 2016) another method combines a foam GO-made, that was able to remove very effectively toxic pollutants as Mercury from water (Henriques et al., 2016). Overall, GO remains unclear and has to be explored in many ways. With the great potential of GO in a very wide future, it is needed to investigate its interaction with different cell types that are in the body and likely to interact with foreign materials.

I.3.4 Potential for Human Exposure

All those properties of GO contribute to increase the use of graphene and its derivatives making them available directly or indirectly in the environment and biological systems. The possibility of release the nanoparticles in a variable environment, may be accidentally or on purpose reach the human body, cause a serious matter where the toxic effect/response in biological systems must be emphasized (Figure 4). A systematic analysis of the potential hazards of graphene and its derivatives is required to be done, as Golkaram, 2015 says carbon based material are either biocompatible or have insignificant toxic effect (Golkaram and van Duin, 2015) but until today it is little known about graphene compared with other carbon nanostructure (Sanchez et al., 2013; Seabra et al., 2014).

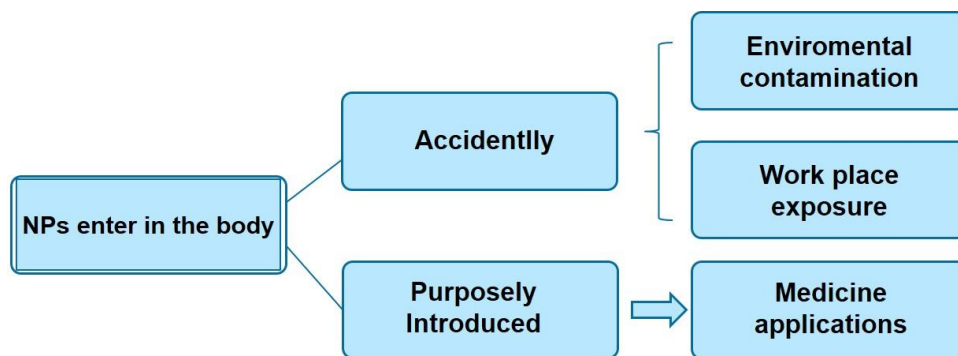


Figure 4. Scheme of general possibility of nanoparticles (NPs) reach the human body.

The knowledge about biocompatibility and toxicity level that graphene or any other nanomaterial might reach in biological system, is important to reach to a degree of safety to its uses. Basically there are four routes to human exposure to nanoparticles: inhalation, intravenous, dermal and oral (Buzea et al., 2007; Love et al., 2012; Sanchez et al., 2013). Therefore, the main routes of exposure in humans is through the skin, lungs, and the gastrointestinal tract. As graphene materials are usually synthesized as dry powders, the inhalation of the material become a significant route to human exposure. The nanomaterial absorption through the several tissues on a biological system may vary, showing a high dependence of the portal of entry and the particle size (Oberdörster et al., 2005) (Figure 5).

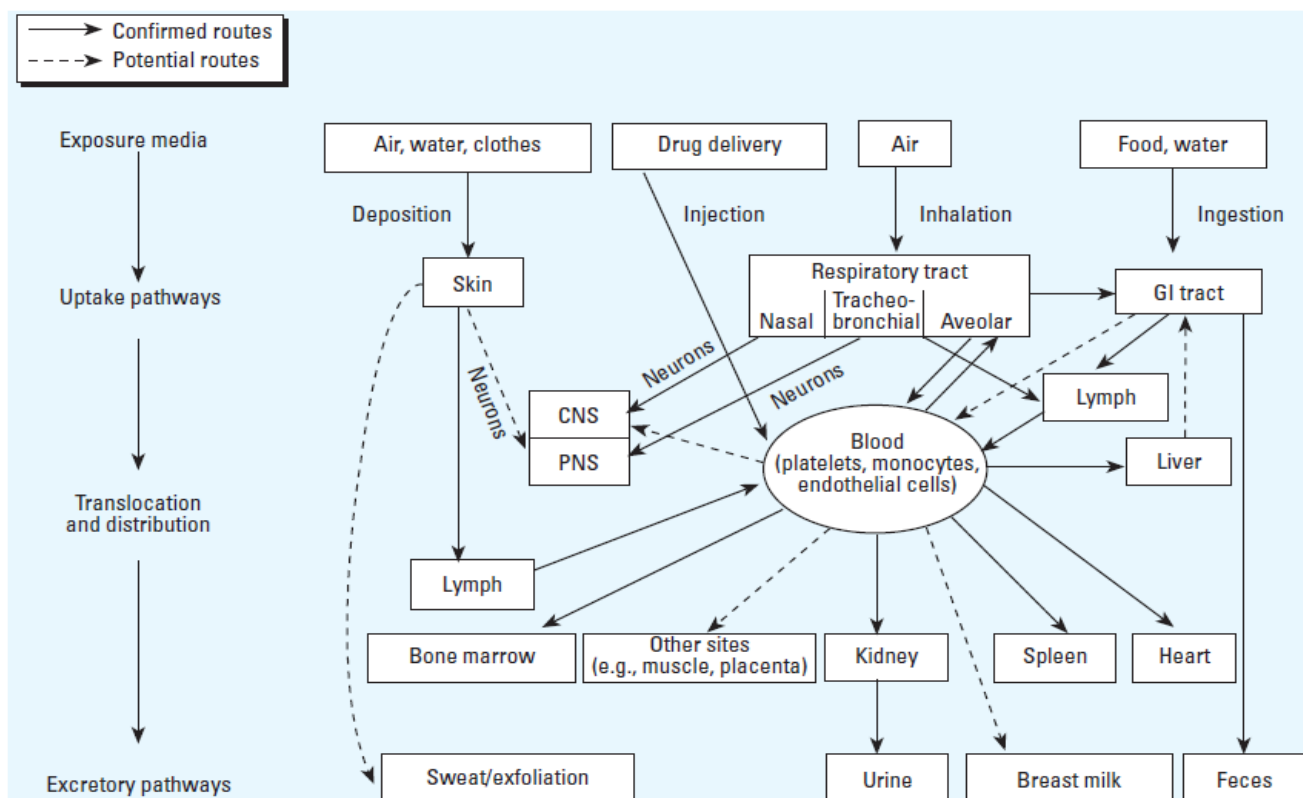


Figure 5. Absorption of Nano-sized particles. Showing routes of exposures, the main uptake pathways, metabolism and excretion of NPS (Oberdörster et al., 2005).

1.4 Nanotoxicity studies

Understanding the potential risks and human impact that are present in the exposure to nanomaterials is the main key for nanotoxicology. This matter leads to an investigation with quantification and visualization methods of nanomaterials *in vitro* and *in vivo* that must be performed with reliable data, trustful tests and protocols (Donaldson et al., 2004). The assessment in nanotoxicology goes above the investigation of routes of exposure, biodistribution, physicochemical and molecular determinants, genotoxicity among other aspects (Donaldson et al., 2004; Lewinski et al., 2008). The main components of risk assessment are the effect and exposure, where the dose-response, bioavailability and bioaccumulation are covered.

The toxicity studies may be divided in different categories: *in vivo*, *in vitro*, *in silico* and/or environmental studies. The most common approaches performed are *in vitro* and *in vivo* studies (Zhou and Gao, 2014). The *in vitro* approach presents some advantages for studying cytotoxicity: as the capacity to determine the primary effects of nanoparticles on target cells, the efficiency, quickness and low cost. On the other way, the *in vivo* study, can take a huge advantage to *in vitro* method since the observation can be performed in a complex organism,

allowing a comparison with the human organism, for example. Still, *in vivo* method must be conducted with monitored parameters, such as: weight change, gastrointestinal function, imaging procedures, mortality, clinical pathology and so on. As much parameters be analysis, more information about the nanoparticles interaction with a complex organism is extracted from the experiment (Adjei et al., 2014). Concerning the *in vivo* experimentation, the ethical approval also is mandatory, despite the existence of various legislature around the world (European Union, 2010) they all aim to comprehend the “3Rs”: designated by replace, reduce and refine which refers to the use of animals for scientific purposes. As proposed by Russell and Burch’s the “3Rs”, the replace means the substitution for conscious living higher animals of insentient material. Reduction means reduction in the numbers of animals used to obtain information of a given amount and precision. Refinement means any decrease in the occurrence or severity of inhumane procedures applied to those animals which still have to be used (Russell and Burch, 1959).

I.5 Toxicity and biocompatibility

As a first step to evaluate the health risks related with nanomaterials, an *in vitro* testing is recommended to investigate the nanoparticle cytotoxicity. The toxicity of GO has also been shown by a number of *in vitro* studies (Chang et al., 2011; Fiorillo et al., 2015; Lay et al., 2013; Liao et al., 2011) and yet it is not clear the degree of the toxicity of GO. Chang et al. (2011) suggested that no obvious toxicity in A549 cell line, however is observed the influence of the nanomaterial size, with the ability to increase the ROS production, it was also confirmed that beyond the size, the shape and aggregation might affect the uptake on the cells (Chang et al., 2011). Another study by Liao and co-workers (2011) reported that even with different cell lines the level of ROS is dose-dependence. A strong dose-dependence is associated with the cytotoxic response (Lay et al., 2013). Additionally it was demonstrated that GO may also confers a selected inhibition to the proliferative expansion of cancer stem cells, Fiorillo et al., 2015 mention that GO treatment, targeted several different signal transduction pathways, reducing overall “stemness”. Taking all into account the applications of GO, a consistent level of studies about the toxicity and human safety level are required (Seabra et al., 2014). Thus wide *in vitro* and *in vivo* studies are essential to explore the biocompatibility and toxicity of the nanomaterial, allowing this way the safe use of GO in clinical applications (Liu et al., 2013).

The limited literature on *in vitro* toxicity suggests that GFNs can be either benign or toxic to cells, and it is hypothesized that the biological response will vary across the material family

depending on layer number, lateral size, stiffness, hydrophobicity, surface functionalization, and dose (Sanchez et al., 2013).

The inhalation route becomes a very significant route to explore, considering the human expose, because of the fact that mostly NPs might entry in the biological system through this route. Inhaled NPs are usually considerably deposited in the human respiratory tract, the distribution, as well as the way of excretion of NPs have been widely studied, among others routes (Figure 5). However, their toxic potential may depend the nanoparticle physico-chemical characteristics (Itoh et al., 2004; Sanchez et al., 2013). Moreover, the damage caused by particle deposition may affect the lung defence and clearance leading to formation of granulomas and lung fibrosis (Card et al., 2008; Itoh et al., 2004). It is also noticed throughout the studies, that *in vitro* cytotoxicity studies of nanoparticles commonly use different cell lines, with variation in incubation times, also a wide range of nanoparticles concentrations are chosen, with different exposure times. All these features make in some way a problem to determinate whether the cytotoxicity observed is physiologically pertinent, and also make a really difficult study to compare the investigations with all these variations (Lewinski et al., 2008).

II. Principles of methods employed

II.1 Characterization of Nanomaterials

Different techniques currently are used to determine the nanoparticle size distribution, concentration and composition in diverse samples. To properly characterize nanoparticles, a number of techniques are recommended such as, UV-Visible Spectroscopy, Dynamic Light Scattering (DLS), Centrifugal Liquid Sedimentation (CLS) Nanoparticle Tracking Analysis (NTA) as well as electron microscopy (EM) techniques (Braakhuis et al., 2015) on the way to allow the possibility to visualize the particle shape and morphology. EM is used to characterize nanoparticles, through Scanning Electron Microscopy (SEM) and Transmission Electron Microscopy (TEM) assays, the average size and size distributions can be measured and calculated by specific software program.

The DLS is a widely used method that uses laser diffraction with multiples scatterings, and can be used to determine the hydrodynamic diameter, as well as the respective agglomeration, in various mediums. DLS is very dependent on the polydispersity of the nanoparticle suspension and also to the material properties of the particles once the scattered light of the individual particles must be strong enough for detection (Chen et al., 2013). This technique allows to measure the size distribution or the average size of molecules and particles dispersed or dissolved in a liquid (Braun et al., 2011).

II.2. In vitro toxicity assessment

There are a number of approaches to assess the *in vitro* toxicity of a nanomaterial, most of them examine on a single, homogeneous, immortal cell type, in a way to reproduce an exposure route on a biological organism, a cell type is chosen. Also, there are two categories to assess nanoparticles toxicity which are the functional assays and viability assays (Love et al., 2012). Frequently, the most of the assays start assessing the viability of cells, while there are others such as, membrane integrity, uptake, oxidative stress, genotoxicity etc. (Kroll et al., 2009; Love et al., 2012).

II.2.1 Cell line and treatment

Considered as an *in vitro* model for type II lung epithelium human cells, A549 cells are commonly employed in lung toxicity assays and has been well-characterized (Foster et al., 1998; Lieber et al., 1976). While the inhalation exposure route is among the most commonly direct way of nanoparticles reach an organism, correlated studies are held in variable assays

such as cell viability and uptake focusing mainly in immortal lung cell lines (Love et al., 2012). The A549 cell line was established in 1972 by D.J. Giard, et al. and it is originated from a Caucasian male, 58 years old, diagnosed with lung adenocarcinoma (Giard et al., 1973). These cells among many features, have the ability to synthesize proteins immunologically related to human surfactant-associated glycoproteins - HSAG (Balis et al., 1984); they also synthesize lecithin (act as a surfactant) with high percentage of disaturated fatty acids (Lieber et al., 1976).

A549 when cultured *in vitro*, grows as an adherently monolayer, show multilamellar cytoplasmic inclusions bodies commonly found in type II lung epithelium human cells (Forbes and Ehrhardt, 2005; Foster et al., 1998; Lieber et al., 1976). When the cells reached the desired confluence on the culture flask to the experiment, they should be submitted to the standard process of detachment, trypsinization. Trypsinization is often used to allow passages or for observation of experimentation. The process of cell dissociation uses trypsin, a proteolytic enzyme to unattached cells from the flasks surface, breaking down proteins (Huang et al., 2010).

II.2.2 Cell Viability

Cell viability is commonly evaluated by using tetrazolium reduction based assays, as well as through the assessment of cell membrane integrity. Among the tetrazolium reduction based assays, the 3-(4,5-dimethylthiazol-2-yl)-2,5-diphenyltetrazolium bromide – MTT is the most commonly used assay to determine cell viability, the principle is mitochondrial activity-based. Other related tetrazolium dyes include the Water-Soluble Tetrazolium salts, as for instance the – WST-8 that works on the same principle but instead of been positive charged as MTT, and therefore able to penetrate viable cells, WST-8 is negatively charged and then not readily penetrates cells. The main difference between the MTT and WST-8 assays, is based on the involved enzymes and solubility. While the WST-8 is water-soluble and the enzymes used are the most of the dehydrogenases, the MTT assay uses only the mitochondria dehydrogenase. WST-8 is reduced by dehydrogenases in cells to give an orange-coloured

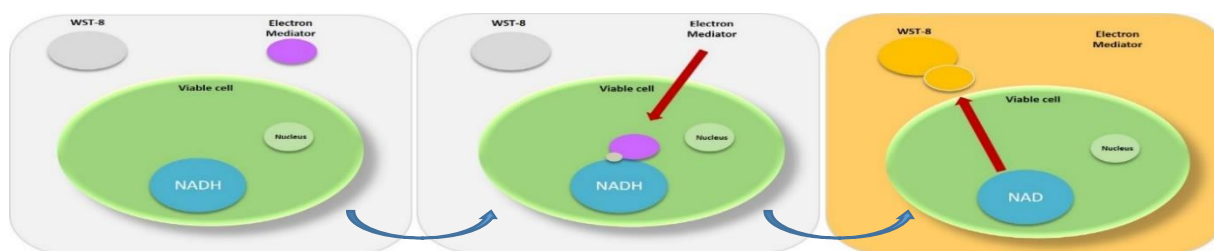


Figure 6. Principle of cell viability detection by WST-8 assay. The WST-8 reagent is added to cells and the electron mediator receives electrons from a viable cell (NADH enzyme) and transfers the electron to WST-8 in the culture medium which is reduced, resulting in an orange-coloured product (formazan).

product (formazan), which is soluble in the tissue culture medium (Figure 6). The amount of the formazan dye generated by dehydrogenases in cells is directly proportional to the number of living cells. WST-8 also does not produce crystals like MTT does, and is achieved by simple steps it determines faster and efficiently viable cell with stability and security.

The WST-8 and MTT solution are colourless, while the result is formazan, a well-stained solution (Held, 2009). The result of MTT is given by a purple formazan in living cell, differently in the WST-8 where the results in a yellow-orange dye. As a recommendable assay, WST-8 is not cytotoxic in the cell culture medium, allowing other test to be done in the same used plate.

Additionally, cell membrane integrity is generally evaluated by the lactate dehydrogenase leakage assay – LDH, and has been used to determine the cytotoxicity of several nanoparticles (Braydich-Stolle, 2005; Chen et al., 2015; Zhang et al., 2012). This assay is based on the amount of lactate dehydrogenase activity in the extracellular medium, the loss of intracellular LDH, demonstrates the cell death due to cell membrane injury (Fotakis and Timbrell, 2006).

Among others assays, there are those that exclude various dye compounds such as Trypan blue, a widely used assay for staining dead cells. In this method, cell viability is determined by counting the unstained cells with a microscope, yet this assay is commonly used to complement others viability assays but somehow is limited, because cannot be used to distinguish healthy cells from others nonhealthy but still alive cells (Liao et al., 2011; Mbeh et al., 2014). Neutral Red (NR) assay, which is also used to measure cell viability is considered a useful assay to detect lysosomal damage, but is suggests to be used complementally with other tests, as a colorimetric assay, it determines the accumulation of NR dye in the lysosomes of viable and uninjured cells (Fotakis and Timbrell, 2006).

II.2.3 Reactive Oxygen Species

The Reactive Oxygen Species (ROS) production can be assessed by various methods but the most widely used are based in permeable fluorescent and chemiluminescent probes (Eruslanov and Kusmartsev, 2010). The fluorescent probe chosen to this work was the 2'-7'-Dichlorodihydrofluorescein diacetate (DCFH2-DA) which is commonly used to measure the redox state of a cell. This probe has several advantages as for instance, is extremely sensitive to changes in the cell redox state, is inexpensive and can be used to follow changes in ROS over time (Royall and Ischiropoulos, 1993). The probe DCFH2-DA, enters the cells and is deacetylated by cellular esterases producing non-fluorescent DCFH2 and diacetate. In the

cytosol DCFH2 is quickly oxidized to fluorescent DCF by intracellular ROS (Eruslanov and Kusmartsev, 2010; Royall and Ischiropoulos, 1993).

II.2.4 Cell cycle analysis

Cell cycle is the biological process and involves different phases. The proliferation of the cells includes four different phases: G₁ phase, where the growth and preparation of the chromosomes happens for the replication; S phase, the synthesis of the DNA take place and the centrosome is duplicate; G₂ phase, is the preparation for Mitosis, which is the final phase (M phase) (Nunez, 2001). Also the cell cycle is regulated on the way to achieve a normal development and to protect the genomic integrity, the regulation process is called cell cycle checkpoints, where several proteins are involved in this process (Bork et al., 2011; Hartwell and Weinert, 1989; Koren, 2007) (Figure 7).

Cell cycle is commonly analysed by flow cytometry (FCM), a powerful method that involves a very precise measurement of DNA content based on the ability to stain the DNA in a stoichiometric manner (Ormerod, 2008). Cell cycle analyses can be also conducted based on the histogram outputs once it plays the distribution of cells in the different phases of the cell cycle (Figure 8).

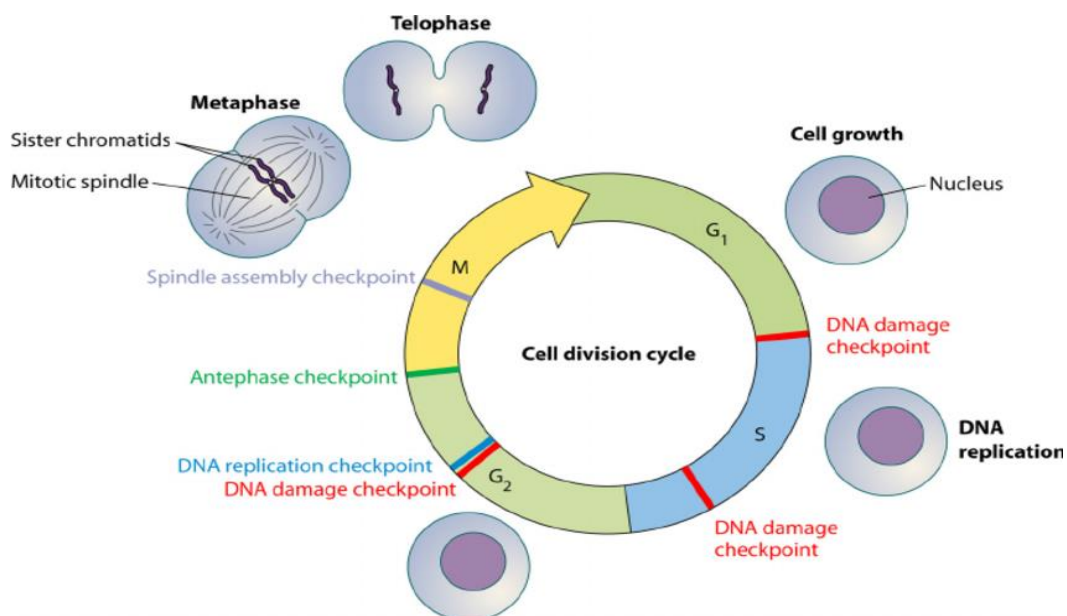


Figure 7. Cell cycle checkpoint pathways impinging upon the cell division cycle. Illustration from Chin and Yeong, 2010.

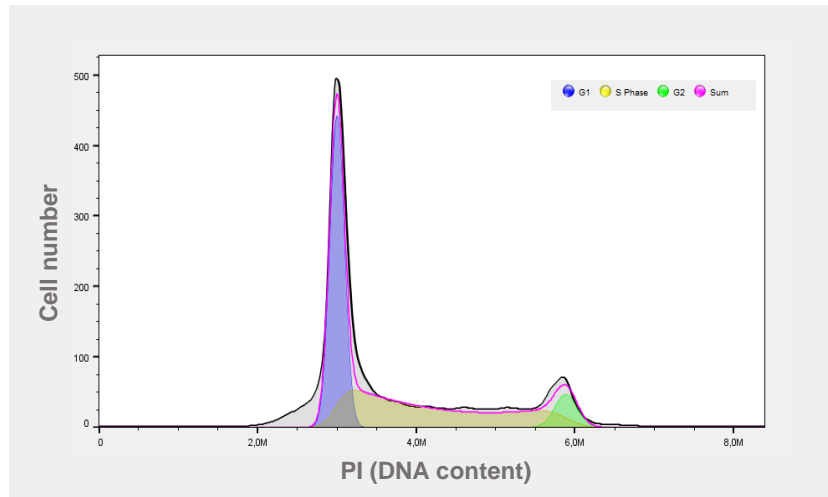


Figure 8. Histogram of cell cycle. Distribution of the cells in different phases of cell cycle.

II.2.5 Flow Cytometry – FCM

Flow cytometry is a system of quantitative single cell analysis, over the time the FCM, especially in the biological area, has become an essential tool to perform important advances in biomedical research, diagnosis, and therapy (Scheffold and Kern, 2000). The equipment consists of five main components: a source of light (laser); a flow cell (where cells are suspended in the sheath fluid); optical components; electronics to amplify and process the resulting signals and finally a computer (Chapman, 2000) (Figure 9).

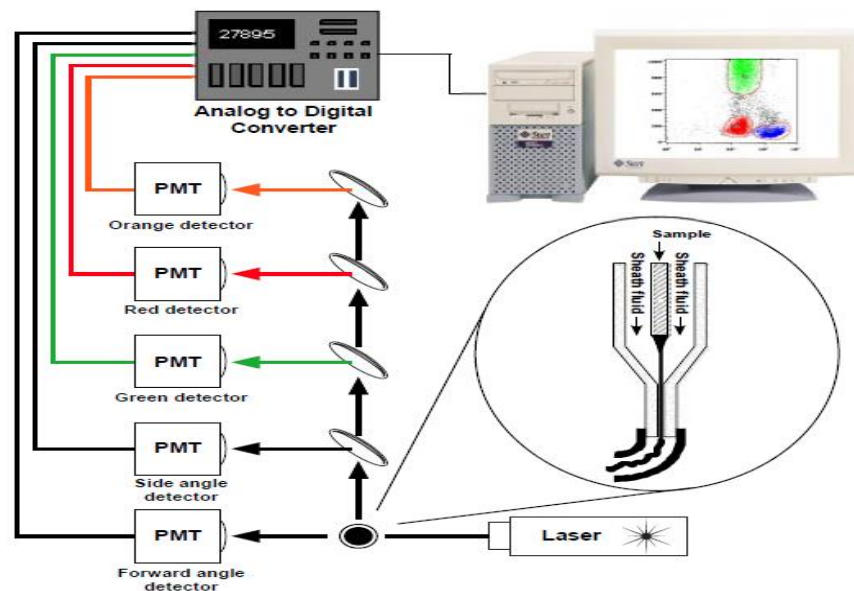


Figure 9. Schematic of a flow cytometer. (Riley and Idowu, 2009)

The power of single cell analysis is the ability to measure multiple parameters simultaneously on each individual cell. The cell shape, surface topography, membrane, nucleus and granular material all affect the scattering of light in the instrument. Light scatter is collected at two angles: forward scatter (FS) and side scatter (SS). Forward scatter is a measurement of the forward direction and is proportional to cell surface area or size. Moreover, SS is collected at approximately 90 degrees from the laser's path and is proportional to cell granularity or internal complexity (Nunez, 2001; Ormerod, 2008). This instrument can perform several kinds of measurements such as cell counting, cell sorting, biomarker detection and protein quantification. In practical way, the mechanism refers as a flow system where the light is focused at the point of measurement. Thereby, the scattered light and fluorescence of different wavelengths are detected by a series of photodiodes and amplified (Ormerod, 2008). While a large diversity of cells is usually analysed in a short period of time, other particles, such as nuclei and chromosomes, can also be studied through FCM, resulting in a quantitative information with valid data about every analysed cell (Chapman, 2000).

III. Aims

The general aim of this study is evaluate the cytotoxicity of graphene oxide in a human lung adenocarcinoma cell line (A549). This cell line, A549 which is commonly used in nanotoxicology studies (Ali-Boucetta et al., 2013; Chang et al., 2011; Fiorillo et al., 2015; Lay et al., 2013) it is seen as a model to *in vitro* studies. Herein, we also highlight that the respiratory track might be one of the main entry point of nano/microparticles into the body.

The specific aims of this work are:

- Characterization of the GO in terms of their physico-chemical properties;
- Evaluate the effects of GO on the cell viability on the human lung adenocarcinoma cell line (A549) using the WST-8 assay;
- Determine the putative ROS induction in A549 cells by GO;
- Evaluate the effects of GO on the cell cycle progression of A549 cells;
- Assess the GO nanoparticle uptake by flow cytometry.

IV. Experimental Procedures

IV.1 Graphene Oxide Material

Graphene oxide (GO) was purchased from Sigma-Aldrich® and the solution was labelled to be dispersed in H₂O (4mg/mL) in a bottle of 50ml. According to product information, GO solution has monolayer sheets in 0.5mg/mL that were assessed by AFM and SEM.

IV.2 Characterization of Graphene Oxide

IV.2.1 Dynamic Light Scattering – DLS

GO was performed by Dynamic Light Scattering (DLS). The hydrodynamic diameter (Dh) and polydispersity index (Pdl) of the particles were measured by dynamic light scattering and the zeta potential was assessed by electrophoretic mobility, both measured experiments of DLS were carried out using a ZetaSizer Nano ZS (Malvern Instruments). Dh was measured in samples diluted in Milli-Q water at final concentration of (10µg/ml). Dh was also measured in samples diluted in complete growth medium (F12-K) at (10µg/ml) and the samples were incubated for 0, 2, 4 and 24 hours. Before the analysis samples were submitted to 2 cycles of 5 minutes of bath sonication (Elmasonic S60H). At the end of the incubation period, samples were placed in standard cuvettes and illuminated by a He-Ne laser at $\lambda=633$ nm. Three scans were set for each measurement. For determination of the zeta potential, GO suspension (10µg/mL, suspended in Milli-Q water) was transferred to a clear disposable zeta cell (Malvern, UK) and after equilibration to a temperature of 25°C for 2 minutes the sample was read. The measurement and runs were determined automatically by the instrument.

IV.3 Cell line culture and treatment

The A549 cell line was used for all the experiments of this study. Cells were cultured in 75 cm² (Corning®) culture flasks in Kaighn's Modification of Ham's F-12 Medium (F-12K) (Gibco), supplemented medium with 10% Fetal Bovine Serum (FBS, Gibco, USA), 1% penicillin-streptomycin (Life Technologies, Carlsbad, CA, USA), and 1% Fungizone (Life Technologies, Carlsbad, CA, USA).

Cells were regularly seen under microscope (Nikon DS-2Mv) to check morphology, confluence and possible contaminants. The subculturing process was done, once the cells reach about 70-80% of the confluence of the flask surface where the old medium was removed, and the cells were washed with phosphate buffered saline – PBS (Gibco). To

detached the cells from the flask or plate was used 0,25% trypsin-ethylenediaminetetraacetate (EDTA) solution as treatment, the cell then were resuspended and counted using a hemocytometer. Finally, the desired number of cells were seed to a new flask with the right proportion of the supplemented F-12K medium. The cells were incubated at 37°C and 5% CO₂. The subculturing process was performed two or three days per week, depending of the required desired confluence. Standard aseptic techniques were followed throughout the experiments.

IV.4 Cell Viability Assay: WST-8

Cell viability was assessed by Cell Counting Kit-8 Assay (Sigma-Aldrich). Preliminary assays were performed in order optimize the WST-8 assay, where different cell densities were chosen and analysed (5×10^3 and 10×10^3 cells/ml) without GO treatment. The incubation time with WST-8 solution was also tested at 1h, 2h, 3h, and 4h.

The protocol of WST-8 was conducted as follow, with some modifications. One hundred μ l of suspended cells at the concentration of 7×10^3 cells/ml, were seeded in 96-well plate and incubated for 24h for adhesion. Once they were adhered, the culture medium was taken out and replaced by 100 μ l of GO in different test concentrations (10, 50, 100, 150 and 200 μ g/ml) in complete growth medium F12-K. Seeded cells in the medium without adding GO were taken as control. After 24h of incubation, the GO-exposed cells and the control were washed with 50 μ l of phosphate buffered saline – PBS (Gibco). Then 100 μ l of complete medium F12-K with 10 μ l of CCK-8 solution were added to each well. The cells were incubated in the normal condition until reading. Lastly, the samples absorbance was measured by a Microplate Reader (Synergy BioTek®– Gen5™ software) at 450nm with blank and background corrections.

In order to check the absorption of culture medium by GO on the toxicity, the protocol described by Chang et al., 2011 was followed with minor modifications. The GO samples (10, 50, 100, 150 and 200 μ l/ml) were incubated in supplemented medium F12-K without cells at the same normal culture condition for 24h. Then, the culture media with GO samples were centrifuged at 5000rpm for 5 minutes to remove most GO. The GO-free supernatants were collected and introduced to A549 cells (7×10^3 cells/well) seeded in the 96-well plate. After 24h of incubation, the cell viability was assessed by WST-8 solution.

IV.5 Determination of Reactive Oxygen Species

The formation of intracellular ROS was measured by using the 2'-7'-dichlorofluorescein diacetate (DCFH-DA) as probe. A549 cells (10×10^4) were seed in 6-well culture plates and allowed to attach for 24 hours in normal condition. Subsequently, the

cells were treated with 10, 50 and 150µg/mL of GO. After 24h of incubation, cells were washed with 1ml of PBS and 1ml of F12K medium containing 10µM of DCFH-DA was added in each a blank sample was provided where no probe was added. Then, the cells were incubated for 30 minutes at 37°C and then washed with 1mL of PBS in order to eliminate the excess of the unreacted probe. The cells were trypsinized and finally collected to cytometry tubes, stored in ice and read in the follow 45 minutes. Flow Cytometry was used to measure the fluorescence of the intracellular reduced DCFH-DA molecules, which is directly related to the intracellular ROS level. Acquisitions were made using Attune® Acoustic Focusing Cytometer (Applied Biosystems). ROS production was estimated from the mean fluorescence intensity of DCF by using the FlowJo software.

IV.6 Cell Cycle Analysis

Cell analysis was evaluated by flow cytometry according to the method described by Oliveira et al., 2014. Cells were seeded (10×10^4) at 6-well plates for 24h in order to allow adherence, at normal culture conditions. Afterwards, culture medium was replaced for the equivalent amount of GO concentrations (10, 50, 150µg/ml), diluted in complete growth medium (F12K) and incubated for 24h. At the end of the exposure period, cells were trypsinized (300µl trypsin-EDTA solution), and transferred to microtubes. The suspensions were centrifuged at 700g during 5 minutes and carefully resuspended in 1ml of cold ethanol 85% for fixation and stored at -20°C until further analysis. To cell cycle analyses, cells were centrifuged at 3000rpm for 6 minutes, resuspended in 800µl of PBS and filtered through a 55 µm nylon mesh to remove big clusters. Subsequently, 50µl of propidium iodide (PI) from Fluka, (USA) and 50µl of RNase were added (Sigma Aldrich, USA) were added to stain nuclear DNA and remove RNA from the samples, respectively. Samples were incubated for 15 minutes in the dark and read in the Attune® Acoustic Focusing Cytometer (Life Technologies). Data was analysis with the FlowJo Software.

IV.7 Intracellular uptake

Intracellular uptake assay was performed following the Suzuki, Toyooka, & Ibuki, 2007 protocol with some adjustments. Cells were seeded (10×10^4) at 6-well plates for 24h in order to allow adherence at the normal culture conditions in three independent assays. Subsequently, culture medium was replaced for the equivalent amount of GO concentrations (10, 50, 150µg/ml), diluted in complete growth medium (F12K) and incubated for 2h, 4h and 24h in different temperatures (4°C and 37°C). At the end of the exposure period, cells were

trypsinized (300µl trypsin-EDTA) and the cell suspension were resuspended and collected to cytometer tubes. The degree of cell uptake or adsorption on to the cell membrane was analysed using forward scatter (FS) vs side scatter (SS) by Attune® Acoustic Focusing Cytometer. Data was analysis with the FlowJo Software.

IV.8 Statistical analysis

Independent assays were performed for each assay. Data were expressed as mean \pm standard deviation (SD). One-way ANOVA was performed using Sigma Plot software, version 12.0 in order to evaluate the statistical significance between the control and the exposed cells, followed by the Dunnet test. Normality was verified by the Shapiro-Wilk test.

V. Results

V.1 Characterization of GO

V1.1 Zeta Potential

The results from zeta potential measurements of GO (Table 2) shows an increase from -41,43mV in water to -8,42mV in F12-K culture medium. As the particles have a negative surface charge by nature, they attract positive charges in both solutions leading to an increase in zeta potential.

Table 2. Zeta Potential of graphene oxide in the culture medium and MilliQ water. The samples were analysed by DLS and the data are expressed as means \pm SD of three different scans.

GO (10 μ g/ml)	ζ (mV)
in MilliQ water	-41.43 \pm 0.87mV
in F-12K	-8.42 \pm 0.12mV

V1.2 Size distribution and Polydispersity Index (Pdl)

DLS was assessed in order to evaluate the size distributions and the values of polydispersity indexes (Pdl) of GO in growth medium and in water. The values of Pdl were above 0.5 in all cases, and after the incubation time was observed an increase on the Pdl, reaching at 24h, 0.922, indicating a high polydispersity of graphene oxide.

DLS measurements for hydrodynamic diameter in complete F12K culture medium were obtained with the lowest concentration of GO (10 μ g/mL) after incubation for 0h, 2h, 4h and 24h (table 3). The particles suspended in water at time 0h, showed only 2 peaks and the size (by intensity) was **1220.15nm** while the average size of GO dispersed in culture medium, exhibited 3 peaks which presented size between **180.84nm** and **399.64nm** with diversity. It was observed an increase on the size distribution from 2h to 24h in the medium (F12K) suspension (figure 10). The Z-average size (by intensity) of GO dispersed in Milli Q water showed only 2 peaks with maximum at **1863.4nm (76%)** and minimum at **576.9nm (24%)** while in the samples dispersed in growth medium, they exhibited 3 peaks in all the measurements (Figure 11). The largest peak, showed in zero hour, was at **832.40nm**, consisted of **~63%** and the two others peaks were **478.1nm (34%)** and **18.4nm (%)** of the total volume (table 3).

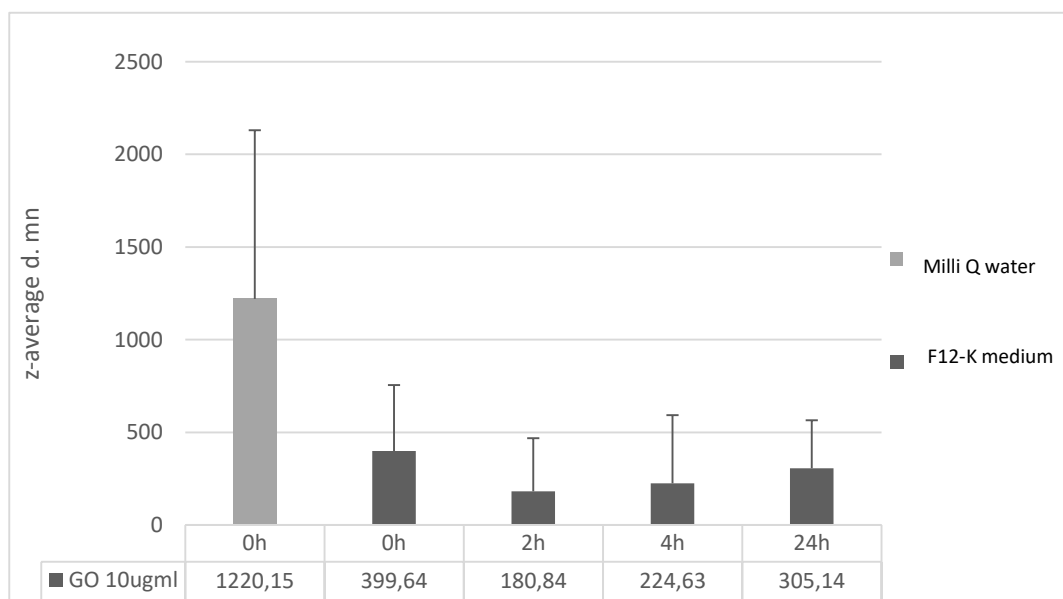


Figure 10. Size distribution of GO (intensity). Samples were suspended in Milli Q water and F12-K medium at concentration of 10µg/ml and assessed by time (0h, 2h, 4h and 24h) the z-average size through DLS. Data are expressed as mean ± SD.

Table 3. Average hydrodynamic diameter (intensity) of GO and the polydispersity index (Pdl) values. Graphene oxide diluted in water and F12-K medium (10µg/mL).

Hydrodynamic diameter (nm)					
Sample	Time	Pdl	Peak 1	Peak 2	Peak 3
MilliQ water	0h	0.595	576.9 nm (24%)	1863.4 nm (76%)	-
F12-K medium	0h	0.730	478.1 nm (34%)	832.4 nm (63%)	18.4 nm (1%)
	2h	0.820	512.8 nm	23.0 nm	6.7 nm
	4h	0.921	649.1 nm (96%)	19.3 nm	5.5 nm
	24h	0.922	428.8 nm	479.4 nm	7.3 nm

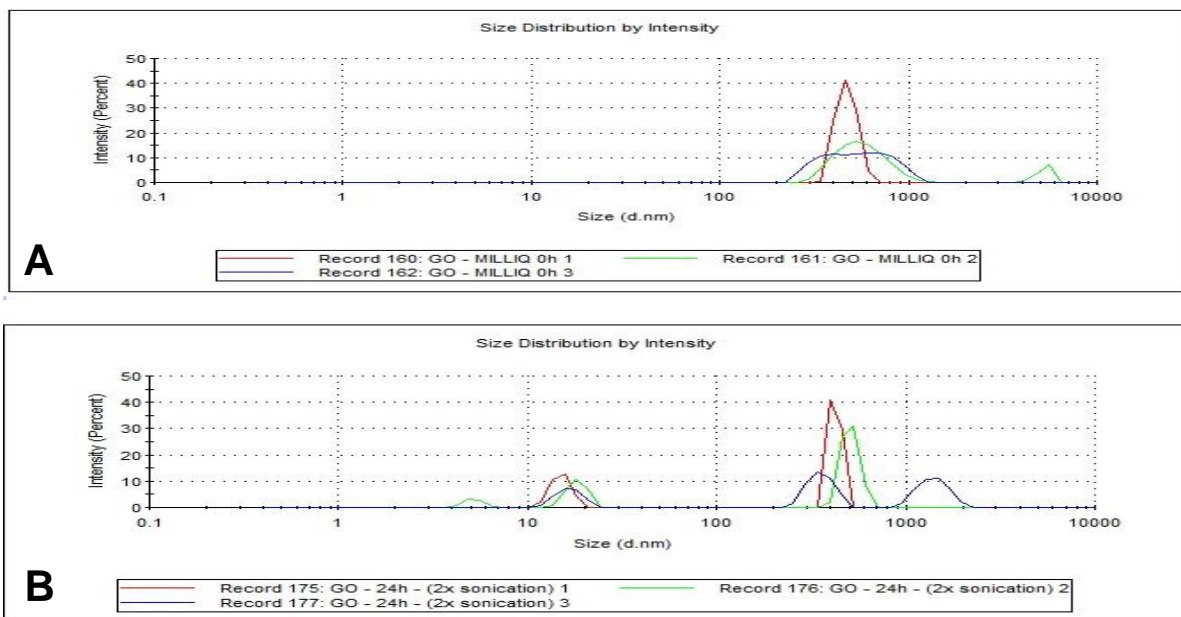


Figure 11. Size distribution (by intensity) report of DLS measurements. **A.** GO dispersion in Milli Q water (0h) and **B.** GO dispersion in F12-K medium.

Size distribution by number was also generated in order to extract more information (Figure 12). As it shows, there is noticeable difference between the water and medium suspension, the size distribution of GO (10 μ g/ml) in Milli Q water was found an average hydrodynamic diameter of **885.4 \pm 147.1nm** while in the growth medium (F-12K) was found an upsurge of the z-average with the increase of the incubation time from **549.8 \pm 134.8nm** at zero hour to **1332.4 \pm 428.2 nm** at 24 hours.

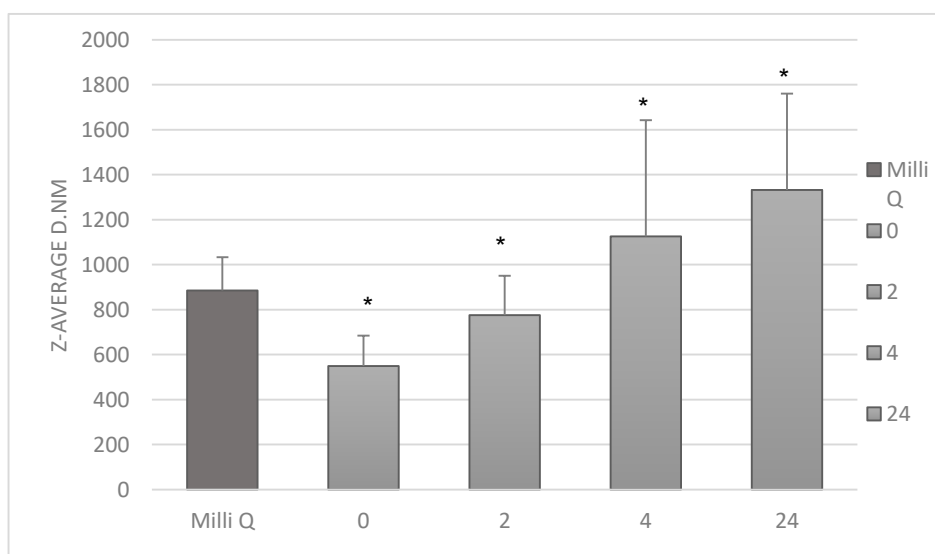


Figure 12. Size distribution (number) of GO in Milli Q water and (*) F-12K medium at concentration of 10 μ g/ml according to incubation time. Data are expressed as means \pm SD.

V.2 Morphology of A549

A549 human lung cancer cells are adherent cells that grow in monolayer and exhibit typical cuboidal epithelial aspect, under normal culture conditions. Once seeded, the cells start to grow in colonies that eventually reach each other; the flask or plate is considered fully confluent when the entire surface is covered with cells (Figure 13).

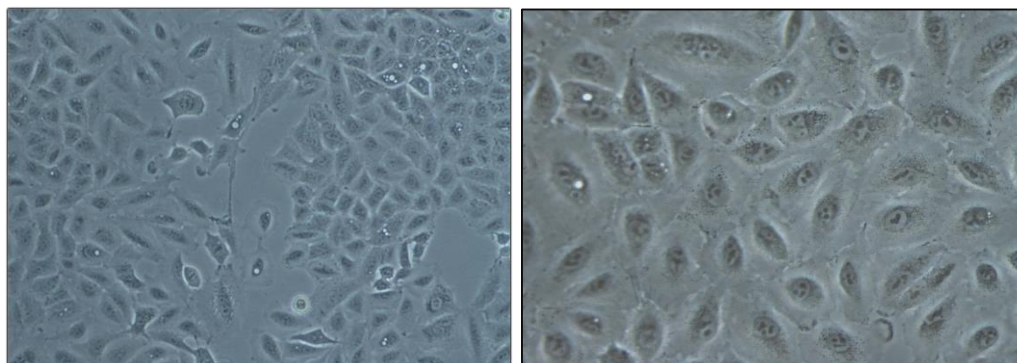
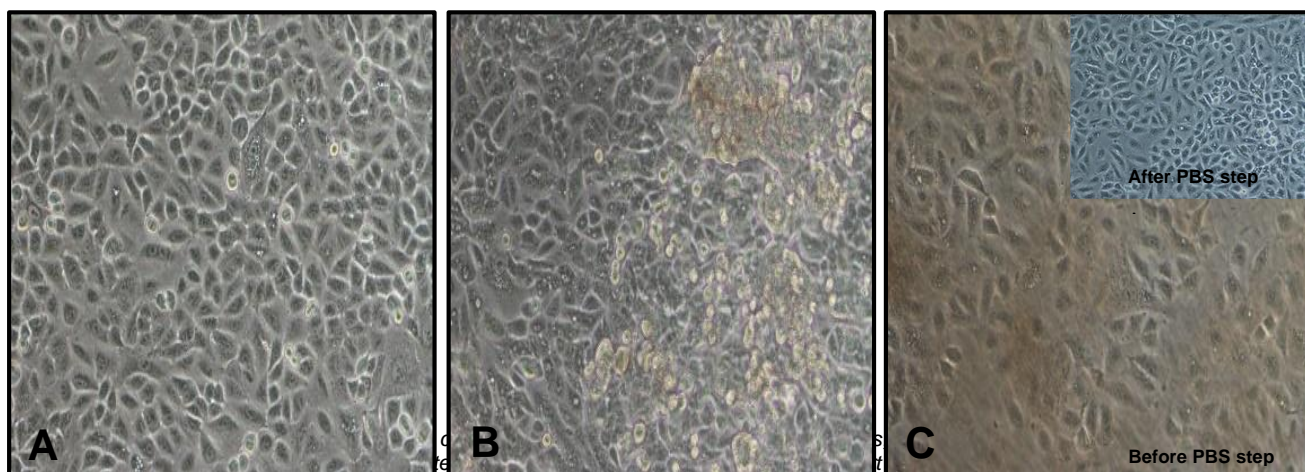


Figure 13. Light microscopy images of A549 cells. Confluence surface of A549 cells; left: cells at 10X magnification; right: cells at 40X magnification.

GO concentrations of 10 $\mu\text{g/mL}$, 50 $\mu\text{g/mL}$, 100 $\mu\text{g/mL}$, 150 $\mu\text{g/mL}$ and 200 $\mu\text{g/mL}$ were chosen to be exposure to A549 cells. After exposure to GO for 24 hours, the cells were observed, and at the lowest concentration (10 $\mu\text{g/mL}$) the cells seem to grow normally but an agglomeration of GO on the medium is observed covering partially the cell surface. The aggregation of GO in the culture medium increases with the rise of GO concentration (figure 14). Regarding the morphology of the cells, after the GO exposure (24h), the cells were observed before and after the washing process with PBS, once all the GO aggregates are rinsed from the well, the normal morphology can be observed, as it shows in Figure 14.C (up right) the GO concentration 150 $\mu\text{g/mL}$ before and after the washing process.



V.3 Cell Viability – WST-8

A preliminary WST-8 assay was performed with different cell densities without GO, in order to find the most suitable cell density (5×10^3 and 10×10^3) and also to select the incubation time (1h, 2h, 3h and 4h) with WST-8 reagent. As shown in the figure 15, the absorbance results through the time and cell densities had different response without any treatment, what shows the increasing of the absorbance, reaching the highest value for both populations at 2h of incubation. The information about the times 3 and 4 hours are not shown, because the absorbance was overflow, meaning the reading was outside of the dynamic range.

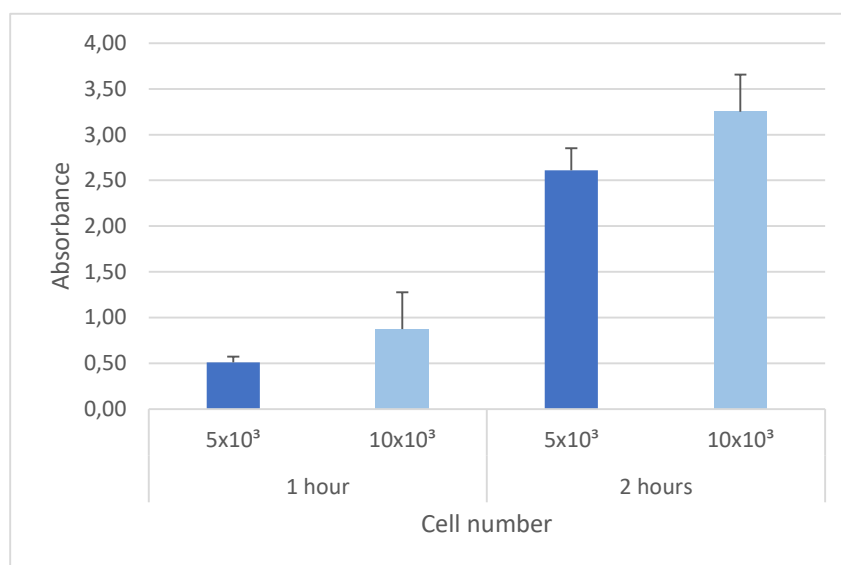


Figure 15. Optimization of WST-8 assay. Performed with 2 cell densities (5×10^3 and 7×10^3); the incubation time were 1h, 2h and 3h and 4 h (data not shown).

The potential cytotoxicity of GO was then evaluated with WST-8 assay in several tests, initially two different cell densities were measured (5×10^3 and 7×10^3), and the 7×10^3 cell density was chosen to be assessed in the following procedures of cell viability.

At the beginning of the study, the WST-8 assay was performed by adding directly the WST-8 solution (10 μ l) to the culture medium with the different concentrations of GO at the different concentrations after 24h, a blank correction and also a background were performed by subtracting the absorbance of the culture medium to the respective GO concentration. The results, showed toxicity response as dose-dependent, reducing the cell viability. A significant reduction of 80% of cell viability was found at the highest concentration (200 μ g/mL) while at the lowest concentration no decrease was found, being almost equal to control cells (figure 16). Also an important observation on the GO behaviour (background samples) was found, regarding GO and the WST-8 reagent. It showed an increase on the absorbance, as is indicated by a green arrow in the figure 16.

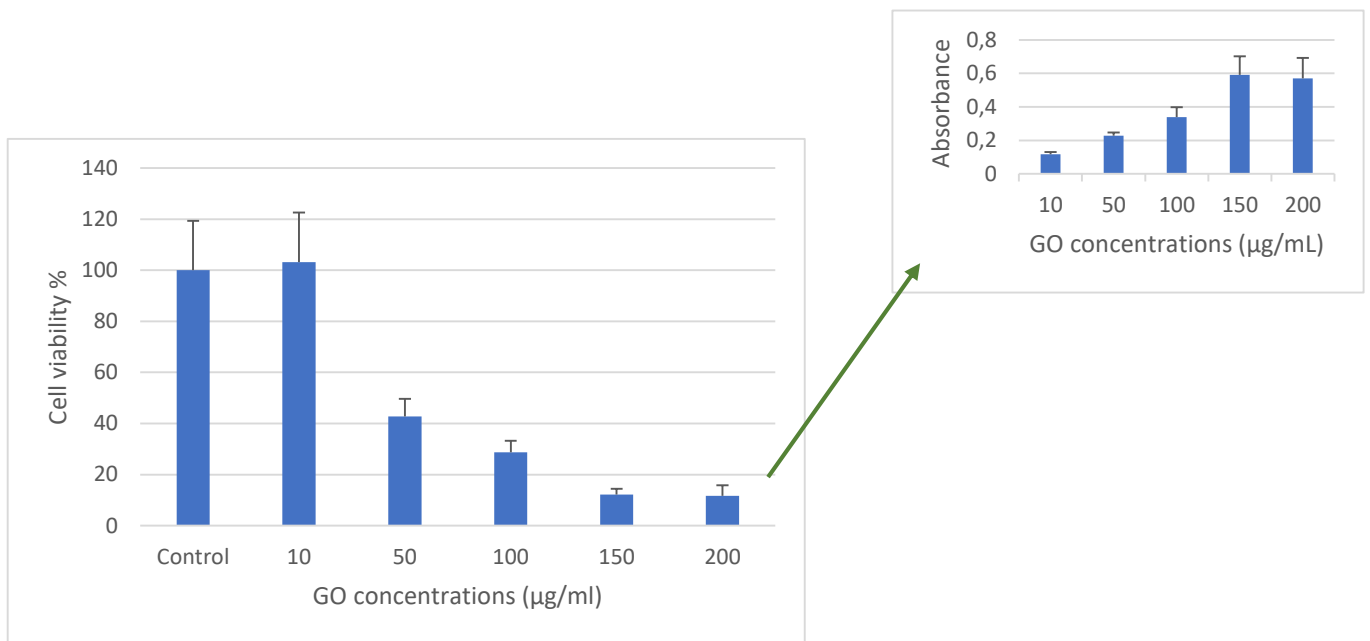


Figure 16. WST-8 assay was performed after A549 cells (7×10^3) were exposed for 24 hours to GO. The cells were not submitted to the PBS washing step in this assays ($n=3$). The green arrow indicates the absorbance found on the GO and WST-8 reagent only. Data is showed as mean \pm SD.

Observing those results, in which the toxicity of GO seems to be overestimated, putatively by an interference of GO with the WST-8 assay. Therefore, in order to reduce that supposed interference, an additional washing step was included to the protocol. In more detail, after the 24h exposure with GO, cells were washed with PBS and after that new culture medium with only WST-8 reagent, was added to all wells. Results of this WST-8 assay are considerably different of the previous ones (Figure 17), in which only a slight decline in cell viability was detected with the increase of GO concentration, but in the highest concentration (200µg/ml) the cell viability was still ~86%, however the differences did not reach the statistical significance.

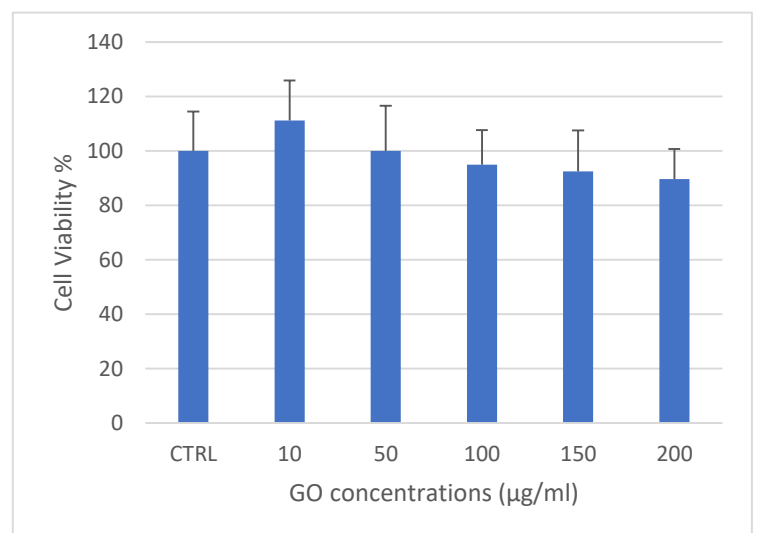


Figure 17. Cell viability of A549 cells exposed to GO in increase concentrations. WST-8 assay was evaluated and statistical analysis was performed with ANOVA. Means \pm SD $n=3$.

In order to evaluate the absorption of culture medium nutrients by GO and if it influences the toxicity, a new set of WST-8 experiments were performed as it is mentioned in the last section. The results did not show any statistically significant difference, however a trend to a decrease in cell viability was observed to the cells exposed to culture medium incubated with GO ($P < 0.05$) (Figure 18).

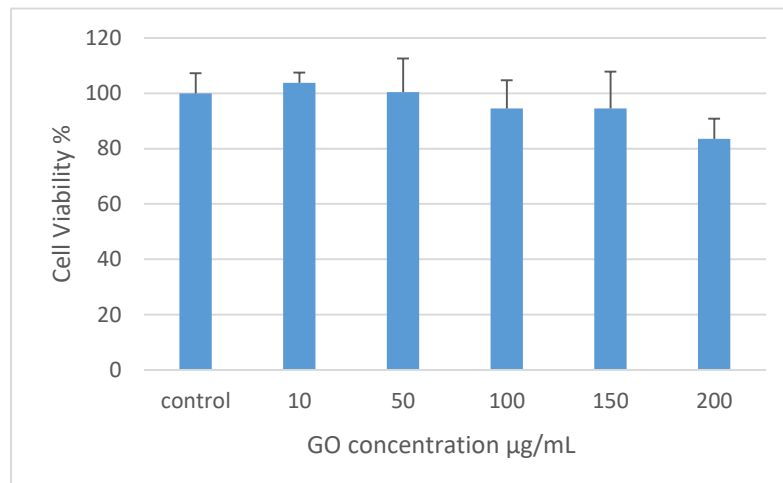


Figure 18. Cell viability assay of A549 cells 7×10^3 exposed to GO-free medium in increase concentrations. WST-8 assay was evaluated and statistical analysis was performed with ANOVA ($p < 0.05$). Means \pm SD $n=2$.

V.4 Determination of Reactive Oxygen Species

The quantification of intracellular ROS in A549 cells exposed to GO for 24h is presented in Figure 19. GO induced the production of ROS reaching a significant 1.6 ±0.19 fold increase at 37µg/mL, compared to control cells. The ROS levels at the highest concentration (150µg/mL) were 0.8 ±0.2 representing a slight reduction compared to control cells. There was a statistically significant difference ($P<0.001$) at 10 and 37µg/mL.

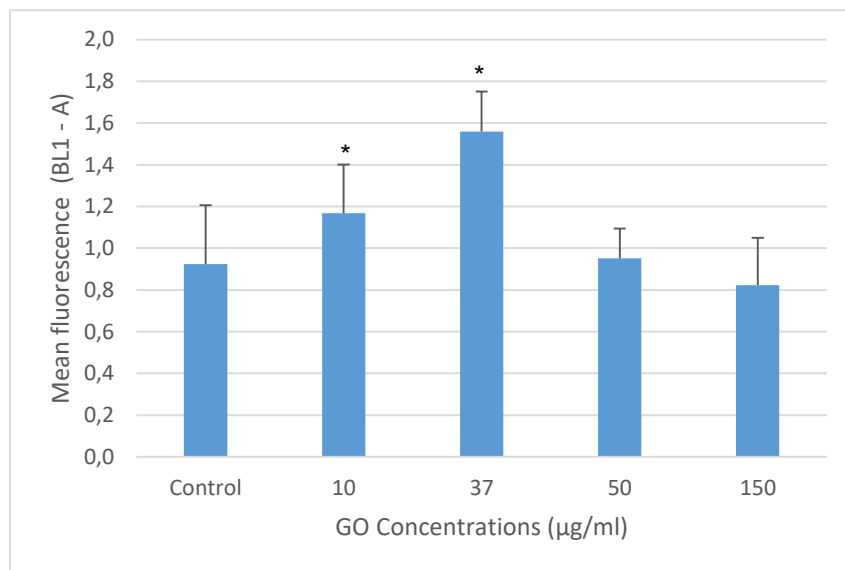


Figure 19. Level of intracellular ROS upon exposure to GO. A549 cells were exposed to increasing concentrations of GO and measured by FCM. (*) shows the statistically significant difference ($P<0.001$). Data shows means ±SD

V.5 Cell Cycle Analysis

After 24h exposure to GO at 10, 37, 50 and 150 $\mu\text{g}/\text{mL}$, A549 cells were collected to perform cell cycle analysis and the global cell cycle stages are showed in figure 20.

The number of counted nuclei was plotted against the intensity of fluorescence detected in BL2-A in the FCM; where the intensity of fluorescence is proportional to the amount of PI bound to the DNA. The boundaries of the peaks were set using the FlowJo software to differentiate nuclei in the G0/G1, S and G2/M phases using the Dean jet Fox model. At concentration 50 $\mu\text{g}/\text{mL}$, a statistically significant decrease in the percentage of cells in S phase and an increase in the percentage of cells in G2 phases was found with $P < 0.001$ (Figure 19).

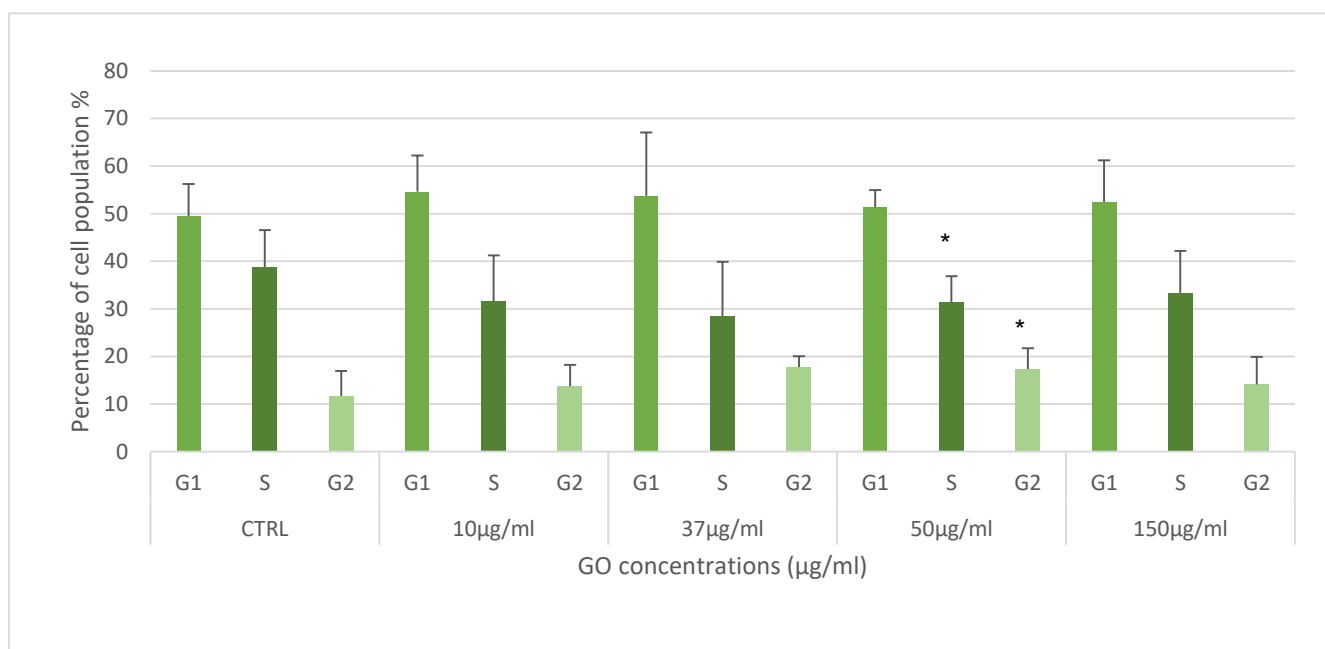


Figure 20. Cell cycle results of A549 GO exposure after 24h. The given results are the mean % of cell population ($\pm\text{SD}$) along cell cycle stages. (*) shows the statistically significant difference ($P < 0,001$) with Multiple comparisons versus control groups.

Exposure to higher lower concentrations of GO did not induce any alterations to the cell cycle of A549 cells, as another way to visualize the results, the figure 21 shows the distribution of the cells, by phase, combining all the GO treatment by phase. Also histograms from the control and GO (50 $\mu\text{g}/\text{mL}$), are shown, as it was the only concentration found a statistically significant difference.

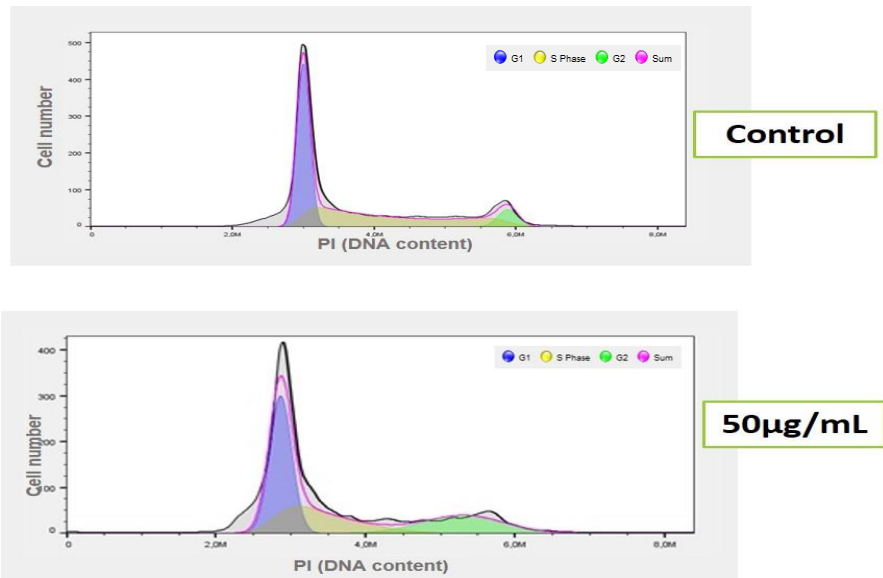
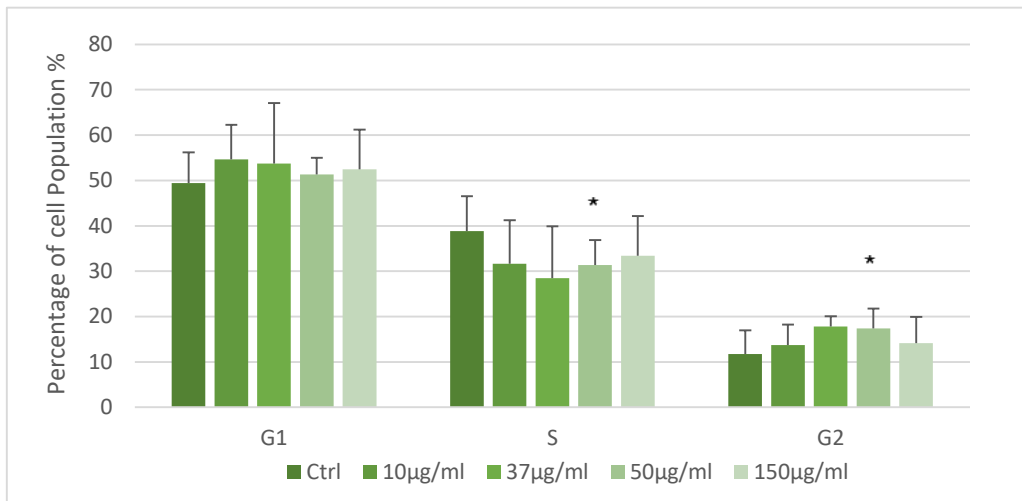


Figure 21. Percentage of cells in each phase of the cell cycle upon exposure to GO for 24h. where (*) shows the statistically significant difference with $P < 0.05$. Histograms are show from control cells and GO (50µg/ml) treated cells.

V.6 Uptake of GO

The uptake of GO was analysed using by evaluating the changes in side scatter (SS) by FCM. Cellular uptake of GO was measured after 2h and 4h incubation at 37°C/4°C and also after 24h incubation at 37°C. The results of 2h of incubation at 37°C showed an increase of SS intensity at 150µg/mL, and statistically significant difference was found ($P<0.05$). When incubated at 4°C, for the same time of incubation (2h) the concentration 50µg/mL exhibited statistically significant difference ($P<0.05$) with a variation in the SS intensity. The results for 24h of incubation at 37°C did not demonstrate any statistically significant difference when compared against the controls (figure 22).

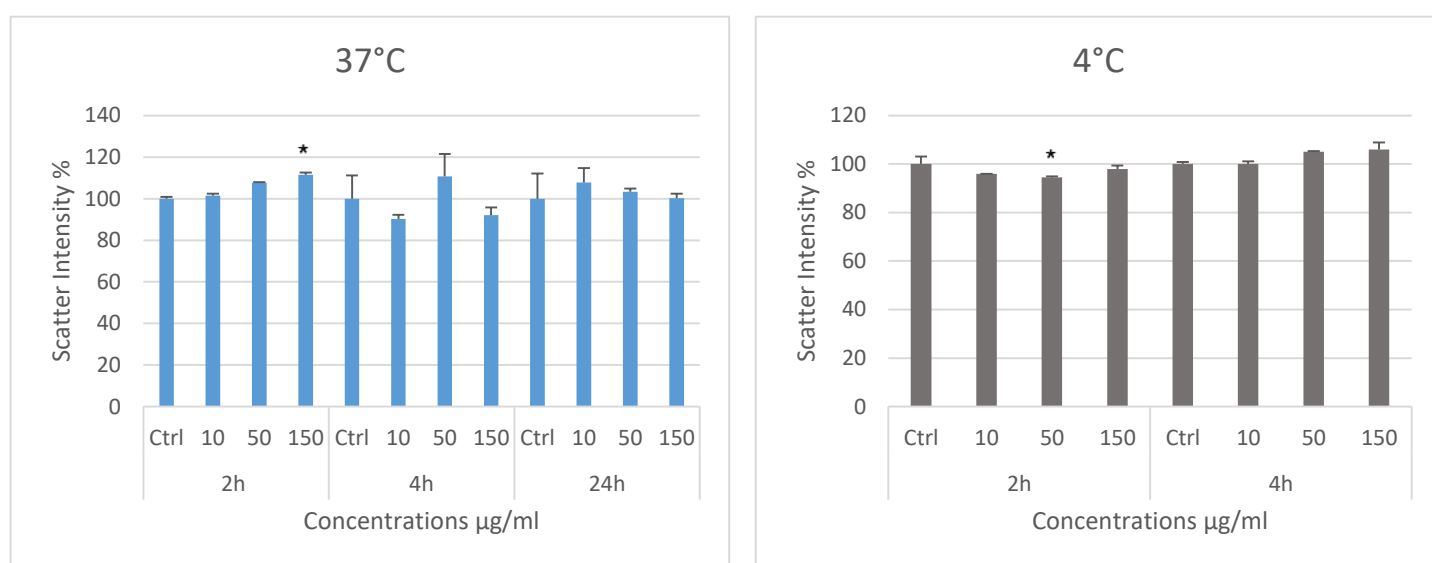


Figure 22. Uptake of GO in A549 cells incubated at 37°C (left hand side) and 4°C (right hand side). (*) shows the statistically significance difference found upon exposure to GO ($P<0.05$). means \pm SD, n=2.

VI. Discussion

Graphene oxide has shown a promising future for many applications in several fields. Once the potential for exposure to nanomaterials has been increasing in the everyday life, the safety level has been an issue to concern, as the behaviour of nanoparticles in biological systems is not yet fully understood. In this study, the cytotoxic potential of the graphene oxide (GO) was assessed in adherent human lung adenocarcinoma cell line (A549), as inhalation is considered one of the main entrance routes of nanoparticles in the organism (Card et al., 2008; Itoh et al., 2004; Sanchez et al., 2013). Therefore, several endpoints were evaluated, namely the cell viability using the WST-8 assay, the production of reactive oxygen species, the cellular uptake and, also, the effects on the cell cycle dynamics. Some studies have already reported the toxicity of GO *in vitro*, in different cell lines, and *in vivo*, however, many inconsistencies in the results were detected.

The zeta potential results show that GO in water carried a strongly negative surface charge (-41.43mV) that considerably increased in F12-K medium towards neutrality, reaching -8.42mV. Since most cellular membranes are negatively charged, the charge of the particle is determinant for the nanoparticle's tendency to permeate membranes. It was also observed that GO in water solution was well dispersed, and that highly negativity found is due to the abundance of carboxyl groups on its surface (Shen et al., 2012). The GO in culture was prone to quick aggregation, due to the low zeta potential, and for that reason samples were bath-sonicated before the measurement of the average hydrodynamic size. After that, a decrease in Dh in time 0 was observed for GO in medium (399.64nm), comparatively to GO in water (1220.15nm). However, the size of GO particles in F12K medium showed a tendency to increase from the 2h to 24h (180.84nm to 305.14nm), showing that GO might increase the average Dh in a biological environment through the time. Knowing that the F12-K is rich in salts, nutrients and most important, electrolytes and chlorides, these components may interfere with size and stability of any nanoparticle. As GO is not a spherical particle, the DLS measurement cannot give accurate results for those particles (Lammel et al., 2013), alternatively electronic microscopy (SEM and/or TEM) could be use in order to characterise the samples.

In order to assess the effect of GO in the cell viability, a range of concentrations of GO were chosen (10µg/mL to 200µg/mL). WST-8 viability assay was performed in A549 cells since this assay is recommended to check the cell viability in carbon nanoparticles (Monteiro-Riviere and Inman, 2006). Moreover, other authors have performed this assay with different cell lines

and graphene nanoparticles such as: erythrocytes and fibroblast (Liao et al., 2011; Wang et al., 2010); breast cancer cell - MCF-7 (Gurunathan et al., 2013); BT-20 (Shim et al., 2015); U87 MG cells (Zhou et al., 2014); human bone marrow neuroblastoma-SK-N-SH and human epithelial carcinoma-HeLa (Chen et al., 2012). Furthermore, Liao et al. 2011 studied the interference between the WST-8 and MTT assays and graphene nanomaterials and found that MTT reacted with the nanoparticles (GO and Graphene sheets) producing MTT purple formazan without cells. Also, the lactate dehydrogenase (LDH) assay was checked in the same study and the test generated underestimation results, leading to a false positive (Liao et al., 2011). A previous study by (Chang et al., 2011) verified viability loss provoked by GO, they selected different sizes (m-GO; s-GO; l-GO) and GO concentrations (10µg/mL from 200 µg/mL), Chang and co-workers, mentioned that the size of the nanoparticle is another factor that will influence cell viability, as in their work, the smallest GO particles were the most cytotoxic, reducing the cell viability in 33% after 24h of exposure. Herein our data, a trend to a dose dependent decrease in cell viability was also observed, however at the highest concentration (200µg/mL) the cell viability was 86% and no statistically significant difference was found. Another relevant study also reported that cell viability can be noticeably reduced as the synthesis method used to produce GO changes (Lay et al., 2013). Lay et al. 2013 assessed the four most common GO preparation methods (oxidative treatments) and the cell viability visibly reduced and showed dose-dependence. The authors reported the relation between the amount of Oxygen-containing groups (C/O ratio) with the loss of viability, as they found, that as higher the amount of C=O, the highest loss of viability and as less amount of C=O, the less cytotoxic effects on the cells.

Regarding the time of exposure, Chang et al. 2011 also comment that for cell viability, time does not seem relevant, as they checked at 24h, 48h and 72h and similar results were found for their experimental conditions (Chang et al., 2011). In this study the chosen time to GO exposure to A549 cells was 24h at all the assessed experiments. The adsorption of the culture medium by GO also was performed to see if the material would be captivating through any way to growth medium after 24h of exposure and no interference was found). Overall, the results did not show any statistically significant difference in the cell viability assay.

To proceed with the next assays, we used a very effective technique, flow cytometry (FCM) which is well recognized for perform measurements with precision and speed, being used for instance to measure oxidative stress, (Amer et al., 2003; Eruslanov and Kusmartsev, 2010) to analyse the cell cycle (Oliveira et al., 2014), and more lately has been used in some

studies to investigate the cellular uptake through the light scattering (side and forward scatter-SS and FS) (Suzuki et al., 2007).

In terms of ROS production, in this study, we explored the generation of ROS using DCFH-DA probe with FCM technique. A complex antioxidant system has been developed to relieve oxidative stress, as a natural ability in biological systems to detoxify the cells, in order to repair a possible damage in the organism, as many studies have demonstrated, oxidation represents a common mechanism to explain the damage of nanomaterials (Adjei et al., 2014; Buzea et al., 2007; Lewinski et al., 2008; Lu et al., 2011; Tang et al., 2015). Thereby, the ROS generation by GO have been evaluated and most of the studies show that this nanomaterial has high potential to induce ROS production even at low concentrations (Chang et al., 2011). Our data confirms that information, when shows a significant increase in ROS levels at the lowest GO concentrations assessed (10ug/mL and 37ug/mL). On the other hand, at the highest concentration of GO (50ug/mL and 150ug/mL) ROS levels decreased to levels similar to the control, suggesting that A549 cells may have neutralized the amount of ROS produced through enzymatic reactions (Liang et al. 2013).

The cell cycle dynamics in terms of percentage of cells in the three main phases (G1, S and G2) was also evaluated by FCM. Our results suggest that GO at 50ug/mL induced alterations in cell cycle dynamics of A549 cells, namely in S phase and G2 phases. Previous studies also observed cell cycle arrest at G2 phase after exposure to carbon nanomaterials (SWCNTs) (Yuan et al., 2011), and alterations in cell cycle dynamics after exposure to GO (Matesanz et al., 2013). The arrest in the G2 phase may indicate that cells are attempting to repair damage or some related misleading of DNA. Then, under the other GO concentrations any significantly changes in cell cycle were detected, even the highest concentration assessed (150ug/mL), which also confirms that GO did not cause any significant toxicity to the cell growth and proliferation (Yan et al., 2012; Yuan et al., 2011). Overall, the slight variations showed in this study on the cell cycle dynamics of GO-treated cells confirms the low cytotoxicity of GO as previously suggested (Ryoo et al., 2010).

Next, in order to evaluate whether the absence of toxicity of GO nanoparticles was due to the inability to readily enter cells, the cellular uptake of GO at 37°C and 4°C was measured by FCM. The cellular uptake in A549 cells showed that there was an increase in the SS intensity found at 150ug/mL concentration with a statistically significant difference comparatively to the control. After the same period (2h) when endocytosis was inhibited (at 4°C) there was a statistically significant difference in the SS intensity for the dose 50µg/ml indicating that the nanoparticles were internalized. In our results, the cellular uptake of GO was not time

dependent, once in a relatively short period of incubation (2h) the SS intensity of the highest concentration of GO was increased.

VII. Conclusion and Future Perspectives

In our study, GO at the range of concentrations tested, did not decrease the viability of A549 cells. However, GO at lower doses may interfere on the ROS production after 24 hours, while at higher doses the ROS levels were similar to those of the control. Concerning the cell cycle dynamics, GO at 50ug/mL induced a decrease in the percentage of cells at S phase and an arrest at G2, what can suggest that the cells are attempting to repair damaged DNA. Our results indicated that the nanoparticles may have been internalized after 2h at 150ug/mL (37°C). In general, GO did not show any obvious toxicity to the cells A549, as morphologically they were considered growing normally after the exposure time, however variations were found in our results and considering the promising applications in a very large range of fields of the material, attention must be taken to further analyse the relationship between graphene oxide and lung cells.

To better understand the physicochemical characteristics of GO in culture medium, future studies should include a more detailed characterization of GO nanoparticles. Furthermore, to fully understand the biological effects of GO to lung cells, future work could entail genotoxicity assessment by, for instance, the evaluation of DNA damage by the comet assay. Finally, considering the role of graphene and its derivatives in the nanotechnology field in the lastly years, the importance of keeping the further investigations with fundamental and experimental research must be highlighted.

VIII. References

- Adjei, I.M., Sharma, B., Labhasetwar, V., 2014. Nanoparticles: Cellular Uptake and Cytotoxicity, in: Capco, D.G., Chen, Y. (Eds.), *Nanomaterial, Advances in Experimental Medicine and Biology, Advances in Experimental Medicine and Biology*. Springer Netherlands, Dordrecht, pp. 73–91. doi:10.1007/978-94-017-8739-0
- Agrawal, D.C., 2013. Introduction, in: *Introduction to Nanoscience and Nanomaterials*. WORLD SCIENTIFIC, pp. 1–8. doi:10.1142/9789814397988_0001
- Ai, J., Biazar, E., Jafarpour, M., Montazeri, M., Majdi, A., Aminifard, S., Zafari, M., Akbari, H.R., Rad, H.G., 2011. Nanotoxicology and nanoparticle safety in biomedical designs. *International journal of nanomedicine* 6, 1117–1127. doi:10.2147/IJN.S16603
- Ali-Boucetta, H., Bitounis, D., Raveendran-Nair, R., Servant, A., Van den Bossche, J., Kostarelos, K., 2013. Purified Graphene Oxide Dispersions Lack In Vitro Cytotoxicity and In Vivo Pathogenicity. *Advanced Healthcare Materials* 2, 433–441. doi:10.1002/adhm.201200248
- Amer, J., Goldfarb, A., Fibach, E., 2003. Flow cytometric measurement of reactive oxygen species production by normal and thalassaemic red blood cells. *European Journal of Haematology* 70, 84–90.
- Balis, J.U., Bumgarner, S.D., Paciga, J.E., Paterson, J.F., Shelley, S.A., 1984. Synthesis of Lung Surfactant-Associated Glycoproteins by A549 Cells: Description of an in Vitro Model for Human Type II Cell Dysfunction. *Experimental Lung Research* 6, 197–213. doi:10.3109/01902148409109248
- Beer, C., Foldbjerg, R., Hayashi, Y., Sutherland, D.S., Autrup, H., 2012. Toxicity of silver nanoparticles — Nanoparticle or silver ion? *Toxicology Letters* 208, 286–292. doi:10.1016/j.toxlet.2011.11.002
- Bork, U., Lee, W., Kuchler, A., Dittmar, T., Thévenod, F., Bork, U., Lee, W., Kuchler, A., Dittmar, T., Thévenod, F., 2011. Cadmium-induced DNA damage triggers G 2 / M arrest via chk1 / 2 and cdc2 in p53-deficient kidney proximal tubule cells Cadmium-induced DNA damage triggers G 2 / M arrest via chk1 / 2 and cdc2 in p53-deficient kidney proximal tubule cells. doi:10.1152/ajprenal.00273.2009
- Braakhuis, H.M., Kloet, S.K., Kezic, S., Kuper, F., Park, M.V.D.Z., Bellmann, S., van der Zande, M., Le Gac, S., Krystek, P., Peters, R.J.B., Rietjens, I.M.C.M., Bouwmeester, H., 2015. Progress and future of in vitro models to study translocation of nanoparticles. *Archives of Toxicology* 89, 1469–1495. doi:10.1007/s00204-015-1518-5
- Braun, A., Couteau, O., Franks, K., Kestens, V., Roebben, G., Lamberty, A., Linsinger, T.P.J., 2011. Validation of dynamic light scattering and centrifugal liquid sedimentation methods for nanoparticle characterisation. *Advanced Powder Technology* 22, 766–770. doi:10.1016/j.apt.2010.11.001
- Braydich-Stolle, L., 2005. In Vitro Cytotoxicity of Nanoparticles in Mammalian Germline Stem Cells. *Toxicological Sciences* 88, 412–419. doi:10.1093/toxsci/kfi256
- Buzea, C., Pacheco, I.I., Robbie, K., 2007. Nanomaterials and nanoparticles: sources and toxicity. *Biointerphases* 2, MR17-R71. doi:10.1116/1.2815690
- Cancino, J., Marangoni, V.S., Zucolotto, V., 2014. NANOTECNOLOGIA EM MEDICINA: ASPECTOS FUNDAMENTAIS E PRINCIPAIS PREOCUPAÇÕES 37, 521–526.
- Card, J.W., Zeldin, D.C., Bonner, J.C., Nestmann, E.R., 2008. Pulmonary applications and toxicity of engineered nanoparticles. *Am J Physiol Lung Cell Mol Physiol* 400–411. doi:10.1152/ajplung.00041.2008.
- Chang, Y., Yang, S., Liu, J., Dong, E., Wang, Y., Cao, A., Liu, Y., Wang, H., 2011. In vitro toxicity evaluation of graphene oxide on A549 cells. *Toxicology Letters* 200, 201–210. doi:10.1016/j.toxlet.2010.11.016

- Chapman, G. V., 2000. Instrumentation for flow cytometry. *Journal of Immunological Methods* 243, 3–12. doi:10.1016/S0022-1759(00)00224-6
- Chen, J.-T., Fu, Y.-J., An, Q.-F., Lo, S.-C., Huang, S.-H., Hung, W.-S., Hu, C.-C., Lee, K.-R., Lai, J.-Y., 2013. Tuning nanostructure of graphene oxide/polyelectrolyte LbL assemblies by controlling pH of GO suspension to fabricate transparent and super gas barrier films. *Nanoscale* 5, 9081–8. doi:10.1039/c3nr02845c
- Chen, L., Hu, P., Zhang, L., Huang, S., Luo, L., Huang, C., 2012. Toxicity of graphene oxide and multi-walled carbon nanotubes against human cells and zebrafish. *Science China Chemistry* 55, 2209–2216. doi:10.1007/s11426-012-4620-z
- Chen, Z., Wang, Y., Zhuo, L., Chen, S., Zhao, L., Luan, X., Wang, H., Jia, G., 2015. Effect of titanium dioxide nanoparticles on the cardiovascular system after oral administration. *Toxicology Letters* 239, 123–130. doi:10.1016/j.toxlet.2015.09.013
- Chin, C.F., Yeong, F.M., 2010. Safeguarding Entry into Mitosis: the Antephase Checkpoint. *Molecular and Cellular Biology* 30, 22–32. doi:10.1128/MCB.00687-09
- Chowdhury, I., Duch, M.C., Mansukhani, N.D., Hersam, M.C., Bouchard, D., 2013. Colloidal properties and stability of graphene oxide nanomaterials in the aquatic environment. *Environmental Science and Technology* 47, 6288–6296. doi:10.1021/es400483k
- Cote, L.J., Kim, J., Tung, V.C., Luo, J., Kim, F., Huang, J., 2010. Graphene oxide as surfactant sheets. *Pure and Applied Chemistry* 83, 95–110. doi:10.1351/PAC-CON-10-10-25
- Donaldson, K., Stone, V., Tran, C.L., Kreyling, W., Borm, P.J.A., 2004. Nanotoxicology. *Occupational and Environmental Medicine* 61, 727–728. doi:10.1136/oem.2004.013243
- Dreyer, D.R., Park, S., Bielawski, C.W., Ruoff, R.S., 2009. The chemistry of graphene oxide. *The Royal Society of Chemistry* 39, 228–240. doi:10.1007/978-3-319-15500-5_3
- Eruslanov, E., Kusmartsev, S., 2010. Advanced Protocols in Oxidative Stress II, *Methods in molecular biology* (Clifton, N.J.), *Methods in Molecular Biology*. Humana Press, Totowa, NJ. doi:10.1007/978-1-60761-411-1
- European Commission, 2011. European Commission Recommendation of 18 October 2011 on the definition of nanomaterial, 2011/696/EU. *Official Journal of the European Union* 54, 275: 38-40.
- European Union, 2010. Directive 2010/63/EU of the European Parliament and of the Council of 22 September 2010 on the protection of animals used for scientific purposes. *Official Journal of the European Union* 33–79. doi:32010L0063
- Fadeel, B., Kasemo, B., Malmsten, M., Strømme, M., 2010. Nanomedicine: Reshaping clinical practice. *Journal of Internal Medicine* 267, 2–8. doi:10.1111/j.1365-2796.2009.02186.x
- Feng, L., Wu, L., Qu, X., 2013. New horizons for diagnostics and therapeutic applications of graphene and graphene oxide. *Advanced materials* (Deerfield Beach, Fla) 25, 168–86. doi:10.1002/adma.201203229
- Fiorillo, M., Verre, A.F., Iliut, M., Peiris-Pagés, M., Ozsvári, B., Gandara, R., Cappello, A.R., Sotgia, F., Vijayaraghavan, A., Lisanti, M.P., 2015. Graphene oxide selectively targets cancer stem cells, across multiple tumor types: implications for non-toxic cancer treatment, via “differentiation-based nano-therapy”. *Oncotarget* 6, 3553–3562.
- Forbes, B., Ehrhardt, C., 2005. Human respiratory epithelial cell culture for drug delivery applications. *European journal of pharmaceuticals and biopharmaceutics : official journal of Arbeitsgemeinschaft für Pharmazeutische Verfahrenstechnik eV* 60, 193–205. doi:10.1016/j.ejpb.2005.02.010

- Foster, K.A., Oster, C.G., Mayer, M.M., Avery, M.L., Audus, K.L., 1998. Characterization of the A549 cell line as a type II pulmonary epithelial cell model for drug metabolism. *Experimental cell research* 243, 359–66. doi:10.1006/excr.1998.4172
- Fotakis, G., Timbrell, J.A., 2006. In vitro cytotoxicity assays: comparison of LDH, neutral red, MTT and protein assay in hepatoma cell lines following exposure to cadmium chloride. *Toxicology letters* 160, 171–7. doi:10.1016/j.toxlet.2005.07.001
- Geim, A.K., 2009. Status and Prospects. *Science* 324, 1530–1534. doi:10.1126/science.1158877
- Geim, A.K., Novoselov, K.S., 2007. The rise of Graphene. *Nature Materials* 6, 183–191. doi:10.1038/nmat1849
- Giard, D.J., Aaronson, S.A., Todaro, G.J., Arnstein, P., Kersey, J.H., Dosik, H., Parks, W.P., 1973. In vitro cultivation of human tumors: establishment of cell lines derived from a series of solid tumors. *Journal of the National Cancer Institute* 51, 1417–23.
- Golkaram, M., van Duin, A.C.T., 2015. Revealing graphene oxide toxicity mechanisms: A reactive molecular dynamics study. *Materials Discovery* 1, 54–62. doi:10.1016/j.md.2015.10.001
- Gurunathan, S., Han, J.W., Eppakayala, V., Kim, J.-H., 2013. Green synthesis of graphene and its cytotoxic effects in human breast cancer cells. *International journal of nanomedicine* 8, 1015–27. doi:10.2147/IJN.S42047
- Hartwell, L.H., Weinert, T.A., 1989. Checkpoints: controls that ensure the order of cell cycle events. *Science (New York, NY)* 246, 629–34. doi:10.1126/science.2683079
- Held, P., 2009. An Absorbance-based Cytotoxicity Assay using High Absorptivity, Water-soluble Tetrazolium Salts - Cell Quantitation Using WST-8 and the Synergy™ Mx. doi:10.1016/j.colsurfb.2009.08.044
- Henriques, B., Gonçalves, G., Emami, N., Pereira, E., Vila, M., Marques, P.A.A.P., 2016. Optimized graphene oxide foam with enhanced performance and high selectivity for mercury removal from water. *Journal of Hazardous Materials* 301, 453–461. doi:10.1016/j.jhazmat.2015.09.028
- Huang, H.-L., Hsing, H.-W., Lai, T.-C., Chen, Y.-W., Lee, T.-R., Chan, H.-T., Lyu, P.-C., Wu, C.-L., Lu, Y.-C., Lin, S.-T., Lin, C.-W., Lai, C.-H., Chang, H.-T., Chou, H.-C., Chan, H.-L., 2010. Trypsin-induced proteome alteration during cell subculture in mammalian cells. *Journal of Biomedical Science* 17, 10–36. doi:10.1186/1423-0127-17-36
- Hummers, W.S., Offeman, R.E., 1958. Preparation of Graphitic Oxide. *Journal of the American Chemical Society* 80, 1339–1339. doi:10.1021/ja01539a017
- Itoh, H., Nishino, M., Hatabu, H., 2004. Architecture of the Lung: Morphology and Function 19, 221–227.
- Jiang, Q., Tian, L., Liu, K.-K., Tadepalli, S., Raliya, R., Biswas, P., Naik, R.R., Singamaneni, S., 2016. Bilayered Biofoam for Highly Efficient Solar Steam Generation. *Advanced Materials* 1–8. doi:10.1002/adma.201601819
- Kiew, S.F., Kiew, L.V., Lee, H.B., Imae, T., Chung, L.Y., 2016. Assessing biocompatibility of graphene oxide-based nanocarriers: A review. *Journal of controlled release : official journal of the Controlled Release Society* 226, 217–228. doi:10.1016/j.jconrel.2016.02.015
- Koren, A., 2007. The role of the DNA damage checkpoint in regulation of translesion DNA synthesis. *Mutagenesis* 22, 155–160. doi:10.1093/mutage/gem003
- Kroll, A., Pillukat, M.H., Hahn, D., Schnekenburger, J., 2009. Current in vitro methods in nanoparticle risk assessment: Limitations and challenges. *European Journal of Pharmaceutics and Biopharmaceutics* 72,

370–377. doi:10.1016/j.ejpb.2008.08.009

- Kuila, T., Bose, S., Mishra, A.K., Khanra, P., Kim, N.H., Lee, J.H., 2012. Chemical functionalization of graphene and its applications. *Progress in Materials Science* 57, 1061–1105. doi:10.1016/j.pmatsci.2012.03.002
- Lammel, T., Boisseaux, P., Fernández-Cruz, M.-L., Navas, J.M., 2013. Internalization and cytotoxicity of graphene oxide and carboxyl graphene nanoplatelets in the human hepatocellular carcinoma cell line Hep G2. *Particle and fibre toxicology* 10, 27. doi:10.1186/1743-8977-10-27
- Lay, E., Chng, K., Pumera, M., 2013. The Toxicity of Graphene Oxides : Dependence on the Oxidative Methods Used. *Chemistry - a European Journal* 19, 8227–8235. doi:10.1002/chem.201300824
- Lewinski, N., Colvin, V., Drezek, R., 2008. Cytotoxicity of nanoparticles. *Small* 4, 26–49. doi:10.1002/sml.200700595
- Li, D., Müller, M.B., Gilje, S., Kaner, R.B., Wallace, G.G., 2008. Processable aqueous dispersions of graphene nanosheets. *Nature nanotechnology* 3, 101–105. doi:10.1038/nnano.2007.451
- Liao, K.-H., Lin, Y.-S., Macosko, C.W., Haynes, C.L., 2011. Cytotoxicity of Graphene Oxide and Graphene in Human Erythrocytes and Skin Fibroblasts. *ACS Applied Materials & Interfaces* 3, 2607–2615. doi:10.1021/am200428v
- Lieber, M., Smith, B., Szakal, A., Nelson-Rees, W., Todaro, G., 1976. A continuous tumor-cell line from a human lung carcinoma with properties of type II alveolar epithelial cells. *International journal of cancer Journal international du cancer* 17, 62–70. doi:10.1002/ijc.2910170110
- Liu, J., Cui, L., Losic, D., 2013. Graphene and graphene oxide as new nanocarriers for drug delivery applications. *Acta biomaterialia* 9, 9243–57. doi:10.1016/j.actbio.2013.08.016
- Liu, Z., Robinson, J.T., Sun, X., Dai, H., 2008. PEGylated Nano-Graphene Oxide for Delivery of Water Insoluble Cancer Drugs (b). *J Am Chem Soc* 130, 10876–10877. doi:10.1021/ja803688x
- Liu, Z., Robinson, J.T., Sun, X., Dai, H., 2008. PEGylated Nanographene Oxide for Delivery of Water-Insoluble Cancer Drugs. *Journal of the American Chemical Society* 130, 10876–10877. doi:10.1021/ja803688x
- Love, S.A., Maurer-Jones, M.A., Thompson, J.W., Lin, Y.-S., Haynes, C.L., 2012. Assessing Nanoparticle Toxicity. *Annual Review of Analytical Chemistry* 5, 181–205. doi:10.1146/annurev-anchem-062011-143134
- Lu, C.H., Yang, H.H., Zhu, C.L., Chen, X., Chen, G.N., 2009. A graphene platform for sensing biomolecules. *Angewandte Chemie - International Edition* 48, 4785–4787. doi:10.1002/anie.200901479
- Lu, X., Qian, J., Zhou, H., Gan, Q., Tang, W., Lu, J., Yuan, Y., Liu, C., 2011. In vitro cytotoxicity and induction of apoptosis by silica nanoparticles in human HepG2 hepatoma cells. *International journal of nanomedicine* 6, 1889–901. doi:10.2147/IJN.S24005
- Lv, Y., Tao, L., Annie Bligh, S.W., Yang, H., Pan, Q., Zhu, L., 2016. Targeted delivery and controlled release of doxorubicin into cancer cells using a multifunctional graphene oxide. *Materials science & engineering C, Materials for biological applications* 59, 652–60. doi:10.1016/j.msec.2015.10.065
- Matesanz, M.-C., Vila, M., Feito, M.-J., Linares, J., Gonçalves, G., Vallet-Regi, M., Marques, P.-A.A.P., Portolés, M.-T., 2013. The effects of graphene oxide nanosheets localized on F-actin filaments on cell-cycle alterations. *Biomaterials* 34, 1562–1569. doi:10.1016/j.biomaterials.2012.11.001
- Mbeh, D.A., Akhavan, O., Javanbakht, T., Mahmoudi, M., Yahia, L.H., 2014. Applied Surface Science Cytotoxicity of protein corona-graphene oxide nanoribbons on human epithelial cells. *Applied Surface Science* 320, 596–601. doi:10.1016/j.apsusc.2014.09.155

- Monteiro-Riviere, N.A., Inman, A.O., 2006. Challenges for assessing carbon nanomaterial toxicity to the skin. *Carbon* 44, 1070–1078. doi:10.1016/j.carbon.2005.11.004
- Nguyen, K.T., Zhao, Y., 2014. Integrated graphene/nanoparticle hybrids for biological and electronic applications. *Nanoscale* 6, 6245–66. doi:10.1039/c4nr00612g
- Novoselov, K.S., Geim, A.K., Morozov, S. V, Jiang, D., Zhang, Y., Dubonos, S. V, Grigorieva, I. V, Firsov, A.A., 2004. Electric Field Effect in Atomically Thin Carbon Films. *Science* 306, 666–669. doi:10.1126/science.1102896
- Nunez, R., 2001. DNA Measurement and Cell Cycle Analysis by Flow Cytometry. *Curr Issues Mol Biol* 3, 67–70.
- Oberdorster, G., 2010. Safety assessment for nanotechnology and nanomedicine: concepts of nanotoxicology. *Journal of Internal Medicine* 267, 89–105. doi:10.1111/j.1365-2796.2009.02187.x
- Oberdörster, G., Oberdörster, E., Oberdörster, J., 2005. Nanotoxicology: An Emerging Discipline Evolving from Studies of Ultrafine Particles. *Environmental Health Perspectives* 113, 823–839. doi:10.1289/ehp.7339
- Oliveira, H., Monteiro, C., Pinho, F., Pinho, S., Ferreira de Oliveira, J.M.P., Santos, C., 2014. Cadmium-induced genotoxicity in human osteoblast-like cells. *Mutation Research - Genetic Toxicology and Environmental Mutagenesis* 775–776, 38–47. doi:10.1016/j.mrgentox.2014.10.002
- Ormerod, M., 2008. Flow cytometry: a basic introduction.
- Park, S., An, J., Jung, I., Piner, R.D., An, S.J., Li, X., Velamakanni, A., Ruoff, R.S., 2009. Colloidal Suspensions of Highly Reduced Graphene Oxide in a Wide Variety of Organic Solvents. *Nano Lett* 9, 1593–1597.
- Perreault, F., Fonseca de Faria, A., Elimelech, M., 2015. Environmental applications of graphene-based nanomaterials. *Chem Soc Rev* 44, 5861–5896. doi:10.1039/C5CS00021A
- Pyrrho, M., Schramm, F.R., 2012. A moralidade da nanotecnologia. *Cadernos De Saude Publica* 28, 2023–2033. doi:10.1590/S0102-311X2012001100002
- Reshma, S.C.C., Syama, S., Mohanan, P.V. V, 2016. Nano-biointeractions of PEGylated and bare reduced graphene oxide on lung alveolar epithelial cells: A comparative in vitro study. *Colloids and surfaces B, Biointerfaces* 140, 104–16. doi:10.1016/j.colsurfb.2015.12.030
- Riley, R.S., Idowu, M., 2009. Principles and Applications of Flow Cytometry 14.
- Royall, J.A., Ischiropoulos, H., 1993. Evaluation of 2', 7'-Dichlorofluorescein and Dihydrorhodamine 123 as Fluorescent Probes for Intracellular H₂O₂ in Cultured Endothelial Cells. *Academic press* 302, 348–355.
- Russell, W., Burch, R., 1959. *The Principles of Humane Experimental Technique*. London.
- Ryoo, S.R., Kim, Y.K., Kim, M.H., Min, D.H., 2010. Behaviors of NIH-3T3 fibroblasts on graphene/carbon nanotubes: Proliferation, focal adhesion, and gene transfection studies. *ACS Nano* 4, 6587–6598. doi:10.1021/nn1018279
- Sanchez, V.C., Jachak, A., Hurt, R.H., Kane, A.B., 2013. Biological Interactions of Graphene-Family Nanomaterials – An interdisciplinary Review. *Chem Res Toxicol* 25, 15–34. doi:10.1021/tx200339h.Biological
- Scheffold, A., Kern, F., 2000. Recent Developments in Flow Cytometry 20, 400–407.
- Seabra, A.B., Paula, A.J., Lima, R. De, Alves, O.L., Dura, N., 2014. Nanotoxicity of Graphene and Graphene Oxide. *Chemical research in toxicology* 27, 159–168. doi:10.1021/tx400385x
- Shan, C., Yang, H., Han, D., Zhang, Q., Ivaska, A., Niu, L., 2009. Water-soluble graphene covalently functionalized by biocompatible poly-L-lysine. *Langmuir* 25, 12030–12033. doi:10.1021/la903265p

- Shen, A.J., Li, D.-L., Cai, X.-J., Dong, C.-Y., Dong, H.-Q., Wen, H.-Y., Dai, G.-H., Wang, P.-J., Li, Y.-Y., 2012. Multifunctional nanocomposite based on graphene oxide for in vitro hepatocarcinoma diagnosis and treatment. *Journal of Biomedical Materials Research Part A* 100 A, n/a-n/a. doi:10.1002/jbm.a.34148
- Shen, H., Liu, M., He, H., Zhang, L., Huang, J., Chong, Y., Dai, J., Zhang, Z., 2012. PEGylated graphene oxide-mediated protein delivery for cell function regulation. *ACS Applied Materials and Interfaces* 4, 6317–6323. doi:10.1021/am3019367
- Shi, J., Wang, L., Zhang, J., Ma, R., Gao, J., Liu, Y., Zhang, C., Zhang, Z., 2014. A tumor-targeting near-infrared laser-triggered drug delivery system based on GO@Ag nanoparticles for chemo-photothermal therapy and X-ray imaging. *Biomaterials* 35, 5847–5861. doi:10.1016/j.biomaterials.2014.03.042
- Shim, G., Lee, J., Kim, J., Lee, H.-J., Kim, Y.B., Oh, Y.-K., 2015. Functionalization of nano-graphenes by chimeric peptide engineering. *RSC Adv* 5, 49905–49913. doi:10.1039/C5RA03080C
- Sun, X., Liu, Z., Welsher, K., Robinson, J.T., Goodwin, A., Zaric, S., Dai, H., 2008. Nano-Graphene Oxide for Cellular Imaging and Drug Delivery. *Nano Res* 1, 203–212. doi:10.1007/s12274-008-8021-8
- Suzuki, H., Toyooka, T., Ibuki, Y., 2007. Simple and easy method to evaluate uptake potential of nanoparticles in mammalian cells using a flow cytometric light scatter analysis. *Environmental Science and Technology* 41, 3018–3024. doi:10.1021/es0625632
- Tang, Y., Shen, Y., Huang, L., Lv, G., Lei, C., Fan, X., Lin, F., Zhang, Y., Wu, L., Yang, Y., 2015. In vitro cytotoxicity of gold nanorods in A549 cells. *Environmental toxicology and pharmacology* 39, 871–8. doi:10.1016/j.etap.2015.02.003
- Wang, K., Ruan, J., Song, H., Zhang, J., Wo, Y., Guo, S., Cui, D., 2010. Biocompatibility of Graphene Oxide. *Nanoscale Res Lett* 6, 8. doi:10.1007/s11671-010-9751-6
- Wu, J., Wang, Y., Yang, X., Liu, Y., Yang, J., Yang, R., Zhang, N., 2012. Graphene oxide used as a carrier for adriamycin can reverse drug resistance in breast cancer cells. *Nanotechnology* 23, 355101. doi:10.1088/0957-4484/23/35/355101
- Yan, L., Wang, Y., Xu, X., Zeng, C., Hou, J., Lin, M., Xu, J., Sun, F., Huang, X., Dai, L., Lu, F., Liu, Y., 2012. Can Graphene Oxide Cause Damage to Eyesight? *Chemical Research in Toxicology* 25, 1265–1270. doi:10.1021/tx300129f
- Yang, X., Zhang, X., Liu, Z., Ma, Y., Huang, Y., Chen, Y., 2008. High-Efficiency Loading and Controlled Release of Doxorubicin Hydrochloride on Graphene Oxide. *The Journal of Physical Chemistry C* 112, 17554–17558. doi:10.1021/jp806751k
- Yuan, J., Gao, H., Sui, J., Duan, H., Chen, W.N., Ching, C.B., 2011. Cytotoxicity Evaluation of Oxidized Single-Walled Carbon Nanotubes and Graphene Oxide on Human Hepatoma HepG2 cells: An iTRAQ-Coupled 2D LC-MS/MS Proteome Analysis. *Toxicological Sciences* 126, 149–161. doi:10.1093/toxsci/kfr332
- Zhang, B., Wang, Y., Zhai, G., 2016. Biomedical applications of the graphene-based materials. *Materials Science and Engineering: C* 61, 953–964. doi:10.1016/j.msec.2015.12.073
- Zhang, X., Hu, W., Li, J., Tao, L., Wei, Y., 2012. A comparative study of cellular uptake and cytotoxicity of multi-walled carbon nanotubes, graphene oxide, and nanodiamond. *Toxicology Research* 1, 62. doi:10.1039/c2tx20006f
- Zhou, R., Gao, H., 2014. Cytotoxicity of graphene : recent advances and future perspective. *WIREs Nanomed Nanobiotechnology* 6, 452–474. doi:10.1002/wnan.1277

Zhou, T., Zhou, X., Xing, D., 2014. Controlled release of doxorubicin from graphene oxide based charge-reversal nanocarrier. *Biomaterials* 35, 4185–94. doi:10.1016/j.biomaterials.2014.01.044